



Supplement of

Observing glacier elevation changes from spaceborne optical and radar sensors – an inter-comparison experiment using ASTER and TanDEM-X data

Livia Piermattei et al.

Correspondence to: Livia Piermattei (livia.piermattei@geo.uzh.ch)

The copyright of individual parts of the supplement might differ from the article licence.

The supplemental materials complement the manuscript by including Figures and Tables that describe the validation data and spaceborne results submitted by the groups. Figure S1-S5 show the airborne validation DEMs of the three study sites, with their respective stable areas, and elevation change maps between the DEMs for the target validation period. Furthermore, the supplementary tables present a summary of the airborne validation data and the processing procedures for Hintereis (Table S1), Aletsch (Table S2), and Vestisen (Table S3). Tables S4–S15 encompass the experiment spaceborne results submitted by each group, outlining the workflows and processing strategies employed. An overview of the validation and spaceborne results is provided for Hintereis (Table S16), Aletsch (Table S17), Vestisen (Table S18), Baltoro (Table S19-S20 for periods 1 and 2, respectively), and the Northern Patagonian Icefield (Table S21-S22 for periods 1 and 2, respectively).

Supplement Figures

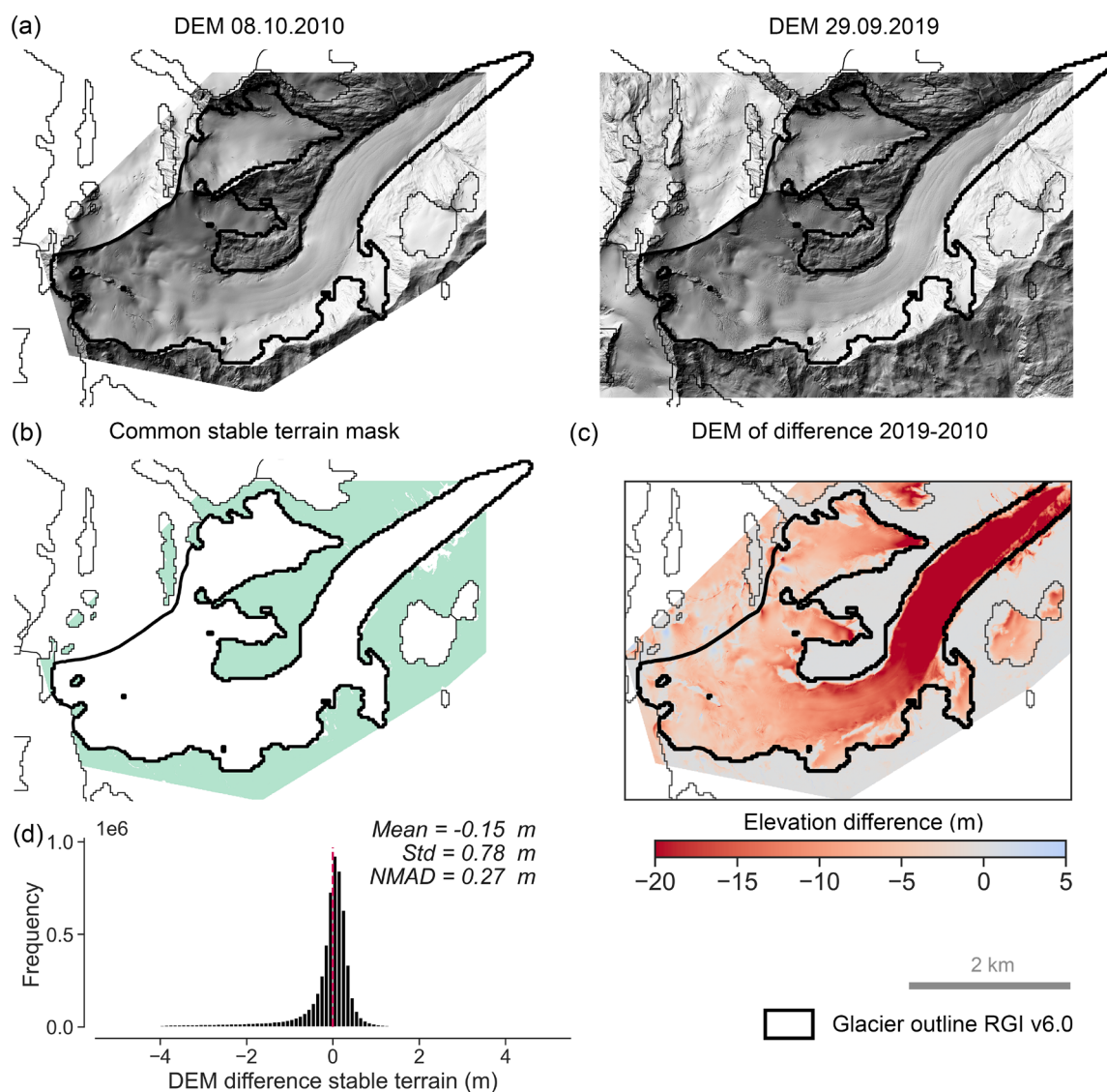


Figure S1: Airborne lidar validation DEM for Hintereis. a) Hillshaded DEMs from 8 October 2010 and 29 September 2019. b) The stable terrain mask common to both DEMs used for co-registration and uncertainty assessment. c) Elevation change in metres between the 2019 and 2010 DEMs and d) the distribution of elevation differences on stable terrain with the main statistics.

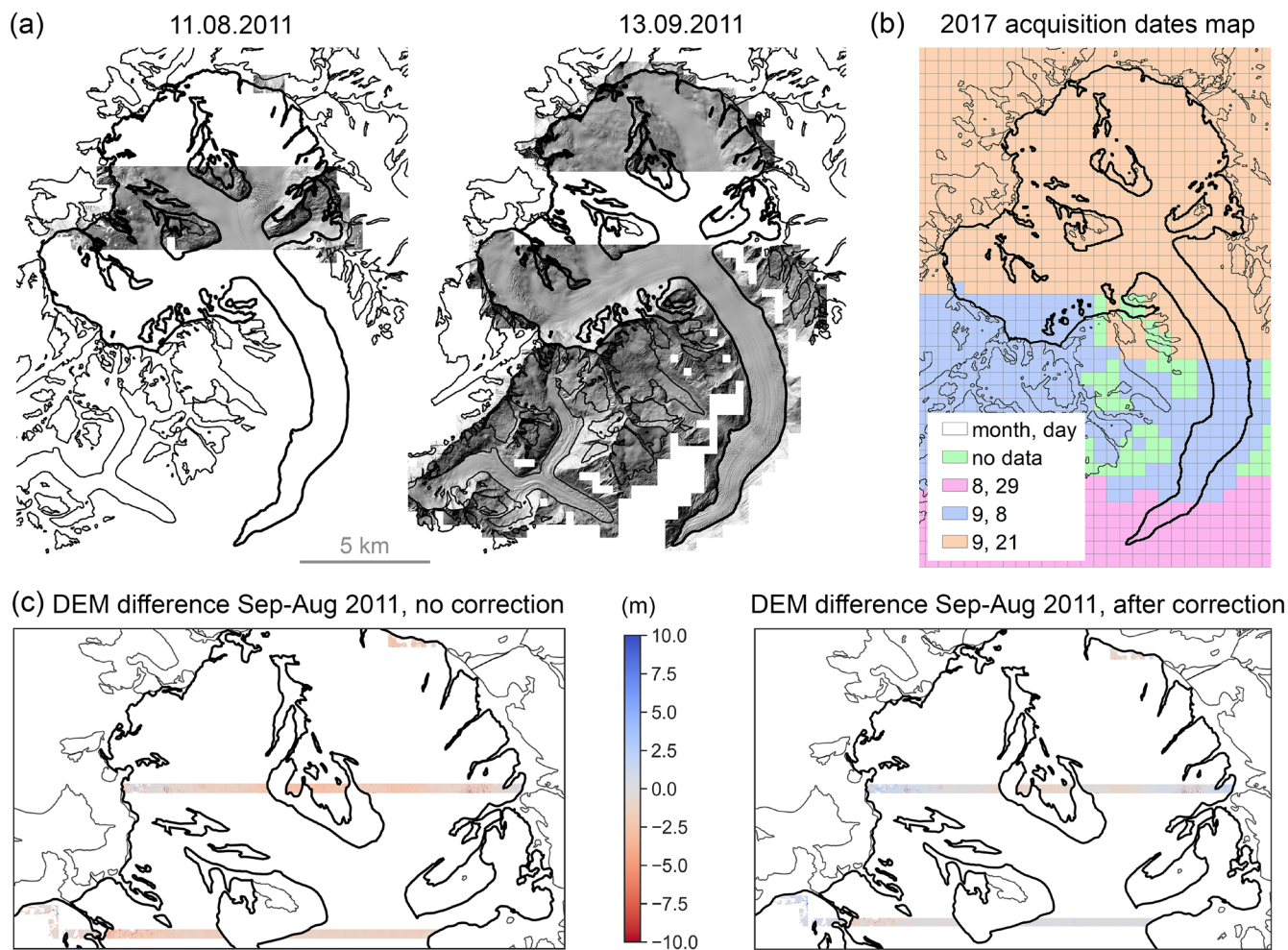


Figure S2: Map of the different acquisition dates of the airborne validation DEMs of Aletsch for the years 2011 and 2017. a) Two overlapping DEM tiles from 11 August 2011 and 13 September 2011. b) A map displaying the acquisition dates of the 2017 airborne flight. c) Elevation differences between September and August 2011 on their overlapping areas, before (left) and after (right) elevation correction (Table S2).

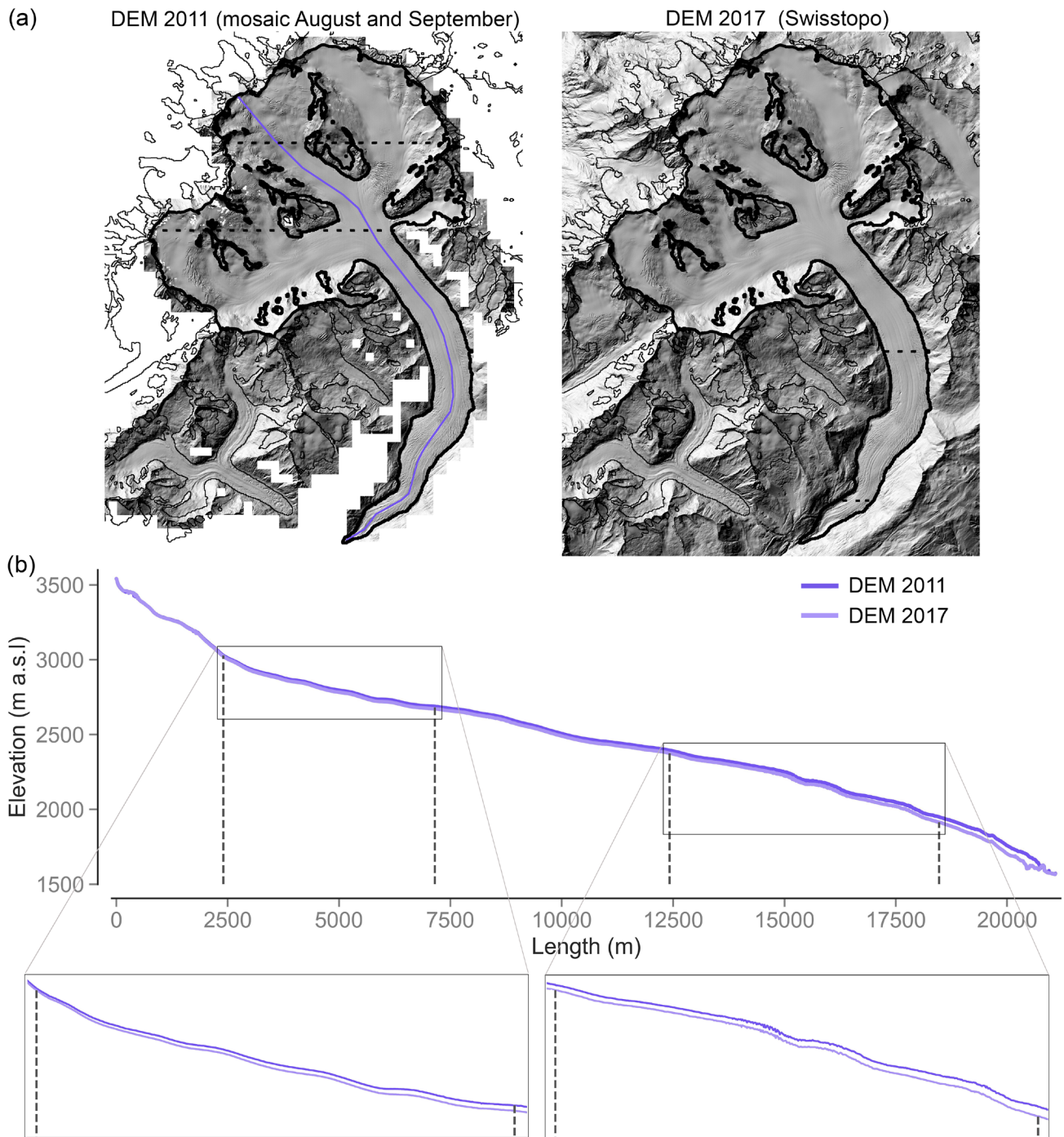


Figure S3: (a) Airborne validation DEMs of Aletsch for 2011 (after correction and mosaic) and 2017, provided by Swisstopo. **(b)** Longitudinal profile along the glacier centreline with dashed black lines indicating the August 2011 DEM location and the 2017 acquisition dates. The inset provides an enlarged view of the DEM profile at the edge of the different survey dates.

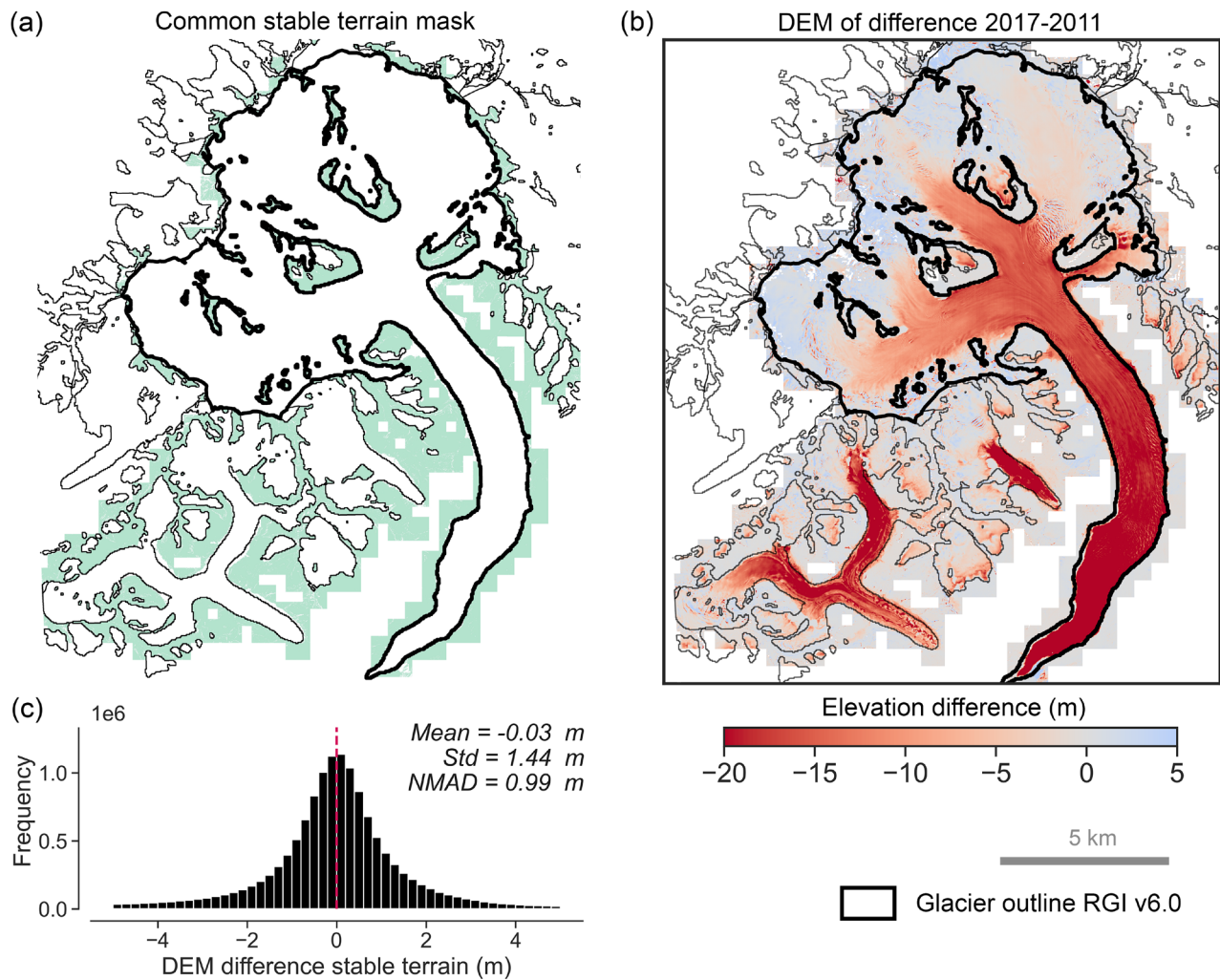


Figure S4: Airborne lidar validation DEM for Aletsch Glacier. (a) The stable terrain mask used for uncertainty assessment and (b) elevation change in metres between the 2017 and 2011 DEMs. (c) The distribution of elevation differences on stable terrain with the main statistics

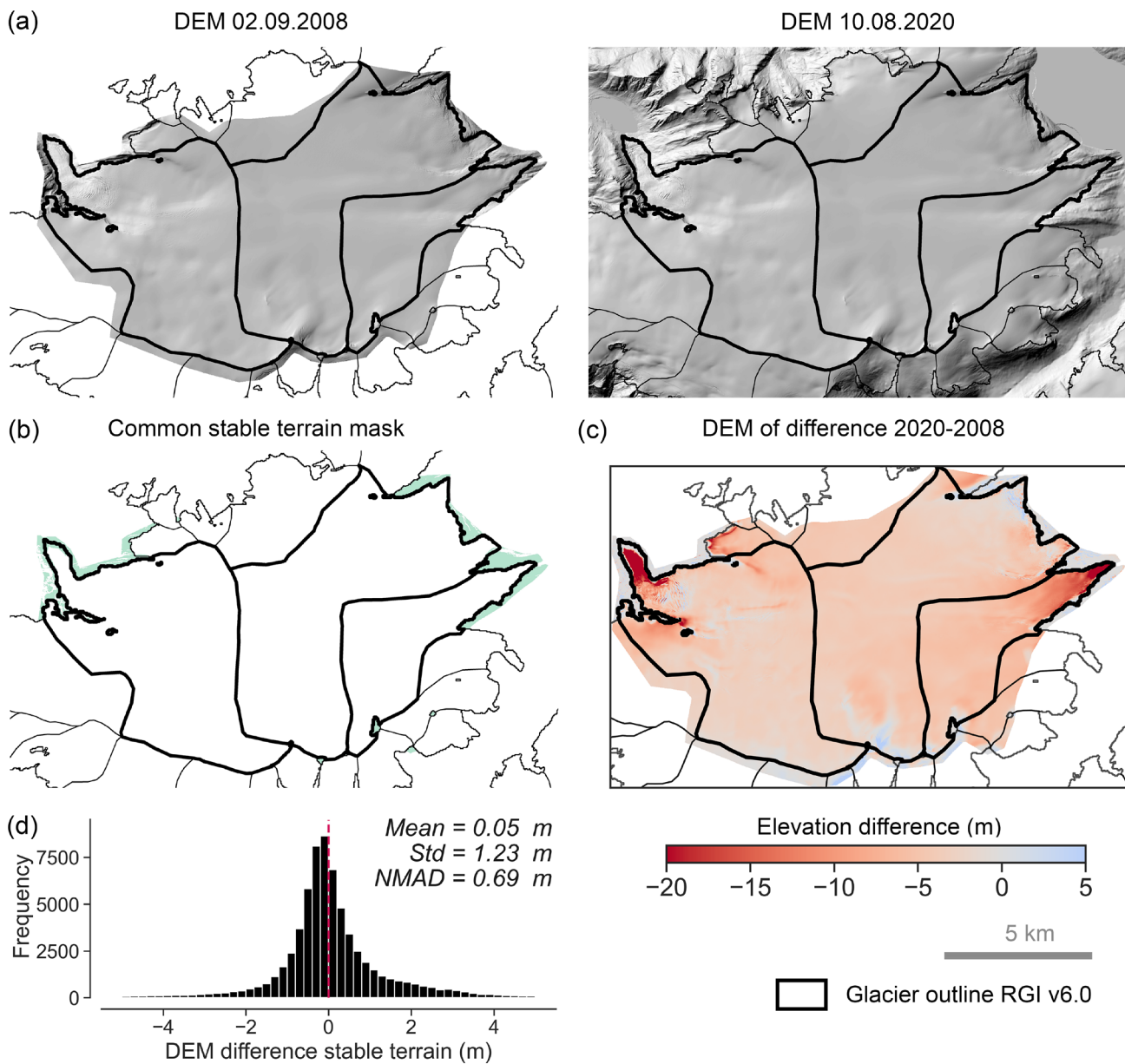


Figure S5: Airborne lidar validation DEM for Vestisen. a) Hillshaded DEMs from 2 September 2010 and 10 August 2020. b) The stable terrain mask common to both DEMs used for co-registration and uncertainty assessment. c) Elevation change in metres between the 2020 and 2008 DEMs and d) the distribution of elevation differences on stable terrain with the main statistics.

Supplement Tables

Table S1. Hintereis airborne validation data

GLACIER NAME	Hintereisferner – Airborne validation data	
ACQUISITION DATE	8 October 2010	21 September 2019
DATA PROVIDER	Christoph Klug and Rainer Prinz University of Innsbruck (AT) (Bollmann et al., 2015):	Florian Siegert, 3D RealityMaps GmbH, München (DE) https://www.realitymaps.de The DEM was created by 3D RealityMaps as a part of the AlpSenseBench Project (2018–2019) and funded by the Bavarian Ministry of Economic Affairs, Regional Development, and Energy.
DEM SOURCE / RESOLUTION	Airborne Lidar, resolution 1 m WGS84 UTM32N, geoid height	Airborne digital photogrammetry, resolution 0.2 m WGS84 UTM32N, geoid height
PROCESSING (dh)	<ul style="list-style-type: none"> • DEM 2019 (reference) resampled to 1 m using bilinear interpolation • Define stable terrain mask for co-registration (Fig. S1b) i.e., the off-glacier area defined by the RGI v6.0, excluding pixels with a difference in elevation (before co-registration) between 2019 and 2010 greater than ± 5 m. • DEM 2010 co-register with DEM 2019. • Elevation difference 2019–2010 DEMs (Fig. S1c). • Noise filtering of stable terrain (off-glacier area) before error assessment. The remaining bias after co-registration is not corrected (mean = -0.15 m, Fig S1d). • Uncertainty estimation on off-glacier area. 	
COREGISTRATION	OpalsLSM (Pfeifer et al., 2014), least squares matching approach, rigid transformation https://opals.geo.tuwien.ac.at/html/stable/ModuleLSM.html	
FILTERING	Filtering only over off-glacier areas for uncertainty assessment due to morphological changes in the periglacial area. Removing pixels with elevation differences between 2019 and 2010 greater than ± 5 m (after co-registration).	
VOID-FILLING	No voids in the original DEMs. Off-glacier voids generated after filtering were not filled	
RADAR PENETRATION	Not applicable	
UNCERTAINTY	Uncertainty of dh at a 95% confidence interval is ± 0.255 m. The details of the error calculations, based on (Pfeifer et al., 2014), are available here: https://github.com/FannyBrun/uncert_RAGMAC_validation/blob/main/uncert_AT_Hintereis_from_Hugonnet_2022.ipynb	
NOTE	The 2010 DEM has a smaller coverage than the RGI v6.0 (7,858 km ² vs 8,036 km ² respectively). Therefore, the DEMdiff 2019–2010 does not cover the RGI outline (Fig. S1a). However, the Lidar DEM 2010 observes the entire glacier, including the glacier tongue, as visible in the hillshade DEM. Since the participants worked with RGI06, we compared their DEM of differences using RGI06 and the lidar 2010 extension, and the estimated differences are in the order of centimetres. This is because the proglacial area is subject to erosion.	

Table S2. Aletsch airborne validation data

GROUP NAME	Grosser Aletschgletscher - Airborne validation data	
ACQUISITION DATES	Tile 1 - 13 Sep 2011 and tile 2 - 11 Aug 2011. The coverage of the two DEMs is shown in Figure S2a. Note that the tile partially overlaps.	21 Sep 2017, 29 Aug 2017, and 8 Sep 2017, as illustrated in Figure S2b.
DATA PROVIDER	Christian Ginzler, WSL, Switzerland	Freely available from Swisstopo
DEM SOURCE / RESOLUTION	Airborne digital photogrammetry, 1 m resolution CH03 LV03 (EPSG 21781).	Airborne digital photogrammetry, 2 m resolution CH1903+LV95 (EPSG 2056).

PRE-PROCESSING SINGLE DEMs	<ul style="list-style-type: none"> DEM tile integration: <ol style="list-style-type: none"> We calculated the elevation difference of the glacier between 2011 August and 2011 September on their overlapping area (Fig. S2c, left). After excluding the presence of an elevation-dependent trend in their elevation difference, we corrected the 2011 August DEM by subtracting the median elevation difference, which was 1.45 m. The elevation difference between August 2011 and September 2011 on their overlapping area after correction is shown in Figure S14c right). The two DEMs (i.e. 2011 September and 2011 August) after elevation correction) were then mosaicked. The mosaic DEM (coordinate system CH03 LV03 (epsg 21781) was projected to CH1903+LV95 (epsg 2056). The 1 m resolution was resampled to a 2 m resolution (bilinear interpolation method) to match the 2017 DEM resolution (Fig. S3a). 	The DEM 2017 (Fig. S3a) was provided by Swisstopo, and no information is available regarding the methods used to combine data from different dates. See section NOTE below.
PROCESSING (dh)	<ul style="list-style-type: none"> Elevation difference 2017–2011 DEMs (Fig. S4b) Define stable terrain mask for uncertainty estimation (Fig. S4a) i.e., the off-glacier area defined by the RGI v6.0, excluding pixels with a difference in elevation between 2017 and 2011 greater than ± 5 m. Uncertainty estimation on off-glacier area based on RGI6.0 	
COREGISTRATION	No co-registration was carried out between the two DEMs based on the distribution of elevation differences on stable terrain (Fig. S4c).	
FILTERING	—	
VOID-FILLING	No void filling was applied.	
RADAR PENETRATION	Not applicable	
UNCERTAINTY	Uncertainty of dh at a 95% confidence interval is ± 0.921 m. The details of the error calculations, based on Hugonnet et al. (2022), are available here: https://github.com/FannyBrun/uncert_RAGMAC_validation/blob/main/uncert_CH_ALE_from_Hugonnet2022.ipynb	
NOTE	Multiple flight campaigns were conducted in 2011 and 2017 to cover the entire glacier. In 2011, images were acquired in August and September, resulting in two separate DEMs. The differences in the overlapping area between these DEMs allowed for corrections and then mosaic. The 2017 DEM is a composite of aerial surveys conducted on various dates in both the accumulation and ablation zones (details in the linked source and Fig. S2b). Unlike the 2011 DEMs, no separate DEMs were available for 2017. Nevertheless, the longitudinal profile of both the 2011 and 2017 DEMs does not exhibit any visible jumps corresponding to the different survey dates (Fig. S3b). https://map.geo.admin.ch/index.html?topic=swisstopo&layers=ch.swisstopo.lubis-luftbilder_schwarzweiss.ch.swisstopo.lubis-luftbilder_farbe.ch.swisstopo.lubis-bildstreifen.ch.swisstopo.images-swissimage-dop10.metadata.ch.swisstopo.swissimage-product.metadata.ch.swisstopo.lubis-luftbilder_infrarot&lang=de&bgLayer=ch.swisstopo.swissimage&layers_timestamp=99991231.99991231...2017.99991231&E=2653281.42&N=1142655.05&zoom=4&layers_visibility=false,false,true,false,false,false&layers_opacity=1,1,1,1,0.7,1&catalogNodes=1430	

Table S3. Vestisen airborne validation data

GROUP NAME	Vestisen Icecap – Airborne validation data	
ACQUISITION DATE	2 Sep 2008	10 Aug 2020
DATA PROVIDER	Liss M. Andreassen and Hallgeir Elvehøy, Norwegian Water Resources and Energy Directorate (NVE), Oslo (NO)/Engabreen and Storglombreen 3pkt 2008, /NDH Svartisen 2pkt 2020, Norwegian Mapping Authority (NO) (https://hoydedata.no/)	

DEM SOURCE / RESOLUTION	Airborne Lidar, resolution 10 m, WGS84 UTM33N ellipsoid height. DEM generated in GIS, las to raster conversion.
PROCESSING (dh)	<ul style="list-style-type: none"> Define stable terrain mask for co-registration (Fig. S5b) i.e., the off-glacier area defined by the RGI v6.0, including the manually digitised off-glacier area around the glacier tongue. Interpolated areas within the off-glacier mask are excluded. DEM 2008 co-register with DEM 2020 (larger extension). Elevation difference 2020–2008 (Fig. S5c). Noise filtering of stable terrain (off-glacier area) before error assessment. The remaining bias after co-registration is not corrected (mean = 0.05 m, Fig S5d). Uncertainty estimation on off-glacier area
COREGISTRATION	OpalsLSM (Pfeifer et al., 2014), least squares matching approach, rigid transformation. https://opals.geo.tuwien.ac.at/html/stable/ModuleLSM.html
FILTERING	—
VOID-FILLING	No voids in the original DEMs. Off-glacier voids generated after filtering were not filled.
RADAR PENETRATION	Not applicable
UNCERTAINTY	Uncertainty of dh at a 95% confidence interval is ± 0.18 m for the entire ice cap. The uncertainty of the three individual glaciers is ± 0.196 m. The details of the error calculations, based on Hugonnet et al. (2022), are available here: https://github.com/FannyBrun/uncert_RAGMAC_validation/blob/main/uncert_NO_Vestisen_from_Hugonnet2022.ipynb
NOTE	Limited stable terrain degrades the robustness of co-registration and uncertainty assessment.

Table S4. BAW spaceborne results.

GROUP	BAW – Bavarian Academy of Sciences and Humanities
AUTHORS and AFFILIATIONS	Anja Wendt¹ ¹ Bavarian Academy of Sciences and Humanities, Munich, Germany
GLACIER	Hintereisferner, Grosser Aletschgletscher
GROUP-#	BAW-1
QUALITY FLAG	—
SOURCE	TanDEM-X
DEM	Provided DEMs
PROCESSING (dh)	Differencing of DEM pairs of the same season
REFERENCE DEM	Copernicus DEM
COREGISTRATION	Horizontal shift correction on stable terrain outside RGI polygons according to Nuth and Kääb (2011)
BIAS	Tilt correction by a 1-degree polynomial + correction of median dh
FILTERING	Outlier filtering for dh > 50 m (70 m for Aletsch)
VOID-FILLING	Hypsometric gap filling in 20 m bins for each glacier individually
RADAR PENETRATION	None, assuming comparable conditions in both DEMs, but included in uncertainty analysis
TEMPORAL	dh/dt (and uncertainty) scaled to the validation period using the number of days.
UNCERTAINTY (dh_sigma)	Error components quadratically added: <ul style="list-style-type: none"> Measurement error: NMAD (Höhle and Höhle, 2009) on bedrock, considering spatial autocorrelation (Rolstad et al., 2009) 50% extrapolation error for gaps Penetration depth error of 1 m in accumulation area in winter acquisitions

Table S5. DLR spaceborne results.

GROUP	DLR – German Aerospace Center						
AUTHORs and AFFILIATIONs	Lukas Krieger¹, Dana Floricioiu¹ ¹ Remote Sensing Technology Institute, German Aerospace Center, Oberpfaffenhofen, Germany						
GLACIER	Hintereisferner						
GROUP-#	DLR-1	DLR-2	DLR-3	DLR-4	DLR-5	DLR-6	DLR-7
QUALITY FLAG	Low confidence: combined ascending and descending pass direction	—	—	Low confidence: combined ascending and descending pass direction	—	—	—
SOURCE	TanDEM-X						
DEM	Processed TanDEM-X DEMs with ITP (Fritz et al., 2011)					Provided DEMs	Processed TanDEM-X DEMs with ITP (Fritz et al., 2011)
	2011-09-24	2011-09-24		2011-09-24	2011-09-24		
	— 2020-09-11	— 2019-02-09		— 2020-09-11	— 2019-02-09		
PROCESSING (dh)	DEM difference						
REFERENCE DEM	Copernicus DEM		Edited TanDEM-X DEM (González et al., 2020)	Copernicus DEM			Edited TanDEM-X DEM (González et al., 2020)
COREGISTRATION	Co-registration is performed during DEM processing (Schweisshelm et al., 2021)			Nuth and Kääb (2011) on stable terrain defined as off-RGI area			
BIAS	Median correction to manually selected flat ice-free areas						
FILTERING	1. Absolute elevating changes > +20.0 m are discarded 2. Absolute elevating changes < -100.0 m are discarded 3. For each pixel, a window size of 11x11 pixels is used to calculate the statistics of the surrounding pixels. A pixel is masked if the following condition is met $abs(center_pix - median(neighbourhood)) \geq 2.0 * std(neighbourhood)$						
VOID-FILLING	Hypsometry of DEMdiff (median, elevation bin 50 m)						
RADAR PENETRATION	—						
TEMPORAL	Linear trend fit to validation period						
UNCERTAINTY (dh_sigma)	<ul style="list-style-type: none"> Co-registration uncertainty calculated as in Abdel et al. (2019) Gap filling errors are accounted for if less than 1000 values are found within one elevation band and the search area is expanded to neighbouring glaciers. Then the uncertainty per pixel is set to $\sigma = MAD(x) * 1.48$ Uncertainties because of area, seasonal correction and signal penetration have not been considered Overall error: the error components are added independently $\sigma_{overall} = \sqrt{\sigma_{coreg}^2 + \sigma_{void}^2}$ All errors are reported at the 95% confidence interval 						

GROUP	DLR – German Aerospace Center					
AUTHORs and AFFILIATIONs	Lukas Krieger¹, Dana Floricioiu¹ ¹ Remote Sensing Technology Institute, German Aerospace Center, Oberpfaffenhofen, Germany					
GLACIER	Grosser Aletschgletscher (ALE)					
GROUP-#	DLR-1	DLR-2	DLR-3	DLR-4	DLR-5	DLR-6
QUALITY FLAG	Low confidence: Results expected to be affected by radar penetration due to mixed use of winter and summer DEMs					—
SOURCE	TanDEM-X					
DEM	Processed TanDEM-X DEMs with ITP (Fritz et al., 2011)			Provided DEMs		
	2011-09-23 2011-08-21 — 2018-01-03			2013-03-21 — 2019-01-01		
PROCESSING (dh)	DEM difference					
REFERENCE DEM	Copernicus DEM	Edited TanDEM-X DEM (González et al., 2020)	Copernicus DEM	Edited TanDEM-X DEM (González et al., 2020)	Copernicus DEM	
COREGISTRATION	Co-registration is performed during DEM processing (Schweissshelm et al., 2021)		Nuth and Kääb (2011) on stable terrain defined as the off-RGI area			
BIAS	Median correction to manually selected flat ice-free areas					
FILTERING	<ul style="list-style-type: none"> • Absolute elevating changes > +20.0 m are discarded • Absolute elevating changes < -100.0 m are discarded • For each pixel, a window with a size of 11x11 pixels is used to calculate the statistics of the surrounding pixels. A pixel is masked if the following condition is met • $abs(center_pix - median(neighbourhood)) \geq 2.0 * std(neighbourhood)$ 					
VOID-FILLING	Hypsometry of DEMdiff (median, elevation bin 50 m)					
RADAR PENETRATION	—					
TEMPORAL	Linear trend fit to validation period					
UNCERTAINTY (dh_sigma)	<p>Co-registration uncertainty calculated as in Abdel et al. (2019)</p> <ul style="list-style-type: none"> • Gap filling errors are accounted for if less than 1000 values are found within one elevation band and the search area is expanded to neighbouring glaciers. Then the uncertainty per pixel is set to $\sigma = MAD(x) * 1.48$ • Uncertainties because of area, seasonal correction and signal penetration have not been considered • Overall error: The error components are added independently $\sigma_{overall} = \sqrt{\sigma_{coreg}^2 + \sigma_{void}^2}$ • All errors are reported at the 95% confidence interval 					

Table S6. ETH spaceborne results.

GROUP	ETH – Eidgenössische Technische Hochschule Zürich
AUTHORs and AFFILIATIONs	Romain Hugonnet ^{1,2,3} ¹ Laboratory of Hydraulics, Hydrology and Glaciology (VAW), ETH Zürich, Zürich, Switzerland ² Swiss Federal Institute for Forest, Snow and Landscape Research (WSL), Birmensdorf, Switzerland ³ University of Washington, Civil and Environmental Engineering, Seattle, WA, USA
GLACIER	Hintereisferner, Grosser Aletschgletscher, Vestisen, Baltoro, Northern Patagonian Icefield
GROUP-#	ETH-1
QUALITY FLAG	—
SOURCE	ASTER
DEM	All daytime ASTER DEMs with less than 99% cloud coverage until 30 September 2019 generated with MMASTER routines (Girod et al., 2017) improved in Hugonnet et al. (2021) and ArcticDEM DEMs above 60°N.
PROCESSING (dh)	What is described below in the following order: <ul style="list-style-type: none"> • Co-registration • Bias correction • Re-co-registration • Filtering • Temporal • Gap-filling
REFERENCE DEM	TanDEM-X global 90 m DEM
COREGISTRATION	Horizontal and vertical following Nuth and Kääb (2011)
BIAS	Cross-track polynomial and along-track sum of sinusoids after 3 by 3 granule stitching, see Girod et al. (2017) and Hugonnet et al. (2021) Supplementary Section 1.
FILTERING	Multi-step spatial and temporal filtering, including iterative temporal Gaussian Process regression, see Hugonnet et al. (2021) in supplementary equations S1 to S7.
VOID-FILLING	A weighted version of the local hypsometric method of McNabb et al. (2019), see Hugonnet et al. (2021)
RADAR PENETRATION	Not applicable
TEMPORAL	Temporal Gaussian Process regression of all filtered elevation, see Hugonnet et al. (2021) Equations 1 and 2.
UNCERTAINTY (dh_sigma)	Two error sources: mean elevation change and area. Main equation: see Hugonnet et al. (2021), Equation 3. <ul style="list-style-type: none"> • Mean elevation uncertainty accounts for heteroscedasticity and spatial correlation of errors in DEMs: see Hugonnet et al. (2022), Equation 18 or Hugonnet et al. (2021), Equations 4–6. • Area uncertainty by multiplying the dh error to a buffer of 15 m: see Hugonnet et al. (2021), Methods.
NOTE	Results are extracted from the closest start and end months in a monthly time series. While this partially mitigates seasonal biases, we show in Hugonnet et al. (2021) that small systematic seasonal elevation errors occur due to co-registration on snow-covered terrain (Fig. S5, Table S3). These systematic errors will affect the estimates provided here for different start and end months, while they do not affect the annual and decadal estimates of Hugonnet et al. (2021).

Table S7. FAU spaceborne results.

GROUP	FAU – Friedrich-Alexander-Universität Erlangen-Nürnberg					
AUTHORS and AFFILIATIONS	Christian Sommer¹, Thorsten Seehaus¹, Philipp Malz¹, Matthias Braun¹ ¹ Institut für Geographie, Friedrich-Alexander-Universität Erlangen-Nürnberg, Erlangen, Germany					
GLACIER	Grosser Aletschgletscher (ALE)		Hintereisferner (HEF)		Vestisen (VES)	
GROUP-#	FAU-1	FAU-2	FAU-1	FAU-2	FAU-1	FAU-2
QUALITY FLAG	—	—	—	—	—	Low confidence: Very low spatial coverage due to poor input DEM quality (voids due to clouds).
SOURCE	Provided DEMs					
DEM	TanDEM-X	ASTER	TanDEM-X	ASTER	TanDEM-X	ASTER
PROCESSING (dh)	DEM (mosaics) differencing					
REFERENCE DEM	SRTM	Copernicus DEM	SRTM	Copernicus DEM	Copernicus DEM	
COREGISTRATION	Nuth and Kääb (2011) on stable terrain (outside RGI)					
BIAS	Iterative vertical deramping on stable terrain (outside RGI)					
FILTERING	Hypsometric 1–99% quantile filter (50 m elevation bins)					
VOID-FILLING	Global hypsometric gap filling (50 m elevation bins)					
RADAR PENETRATION		Not applicable		Not applicable		Not applicable
TEMPORAL	—					
UNCERTAINTY (dh_sigma)	SD of stable terrain (outside RGI areas), aggregated in 5° slope bins, weighted by respective glacier area, integration of spatial autocorrelation (Rolstad et al. 2009).					

GROUP	FAU – Friedrich-Alexander-Universität Erlangen-Nürnberg					
AUTHORS and AFFILIATIONS	Christian Sommer¹, Thorsten Seehaus¹, Philipp Malz¹, Matthias Braun¹ ¹ Institut für Geographie, Friedrich-Alexander-Universität Erlangen-Nürnberg, Erlangen, Germany					
GLACIER	Baltoro (BAL) 2000–12 [FAU-1 – FAU-5] 2012–19 [FAU-6 – FAU-10]					
GROUP-#	FAU-1 & FAU-6	FAU-2 & FAU-7	FAU-3 & FAU-8	FAU-4 & FAU-9	FAU-5 & FAU-10	
QUALITY FLAG	—	—	—	—	—	
SOURCE	Provided DEMs					
DEM	TanDEM-X					ASTER
PROCESSING (dh)	DEM (mosaics) differencing					

REFERENCE DEM	SRTM		Copernicus DEM
COREGISTRATION	Nuth and Kääb (2011) on stable terrain (outside RGI)	—	Nuth and Kääb (2011) on stable terrain (outside RGI)
BIAS	Iterative vertical deramping on stable terrain (outside RGI)	—	Iterative vertical deramping on stable terrain (outside RGI)
FILTERING	Hypsometric 1–99% quantile filter (50 m elevation bins)	—	Hypsometric 1–99% quantile filter (50 m elevation bins)
VOID-FILLING	Global hypsometric gap-filling (50m elevation bins)		Global hypsometric gap-filling (50m elevation bins)
RADAR PENETRATION	—		Not applicable
TEMPORAL	—		
UNCERTAINTY (dh_sigma)	SD of stable terrain (outside RGI areas), aggregated in 5° slope bins, weighted by respective glacier area, integration of spatial autocorrelation (Rolstad et al. 2009).		

Table S8. GAC spaceborne results.

GROUP	GAC – Gustavus Adolphus College
AUTHORS and AFFILIATIONS	Laura Boehm Vock¹ and Jeff D La Freniere² ¹ Department of Mathematics, Statistics, and Computer Science, St. Olaf College, Northfield, Minnesota, USA ² Department of Environment, Geography, and Earth Sciences, Gustavus Adolphus College, St. Peter, Minnesota, USA
GLACIER	Baltoro (BAL)
GROUP-#	GAC-1
QUALITY FLAG	—
SOURCE	TanDEM-X
DEM	Provided DEM time series
PROCESSING (dh)	DEM difference
REFERENCE DEM	Copernicus DEM
COREGISTRATION	Co-register all TanDEM-X DEMs to Copernicus DEM as reference DEM following Nuth and Kääb (2011)
BIAS	Find median dh in 50m bins on stable terrain (off-glacier, slope < 40 degrees). Use a linear fit to estimate bias on elevation between 3400–5800 m. For elevation >5800 m, use bias at 5800 m, and for elevation <3400 m, use bias at 3400 m
FILTERING	Removed values exceeding ± 3 NMAD from median elevation in 50 m bins. (areas <3400 m and >5400 m were treated as one bin each due to small values>)
VOID-FILLING	Filled missing pixels with mean dh according to 50m elevation bins
RADAR PENETRATION	We applied an elevation-dependent C-Band penetration model to the SRTM data set based on results specific to East Karakoram by Kumar et al. (2019). We then applied an X-Band radar penetration model to the TanDEM-X tiles collected in the months of January and February based on C/X band penetration differences calculated for the Karakoram region by Lin et al. (2017).

TEMPORAL	—
UNCERTAINTY	<p>We estimate the standard deviation for the different error sources and add them together using propagation of error laws.</p> <p>We report uncertainty as a standard error by dividing it by the square root of the effective sample size (N_{eff}), accounting for spatial correlation, as in Rolstad et al. (2009). Our estimated spatial range parameters for the control results were 270–320 km.</p> <p>The uncertainties accounted for are:</p> <ul style="list-style-type: none"> • Uncertainty in elevation change, dh, measured as standard deviation (denoted σ_{dz}) • Uncertainty due to filing procedure: We did filling based on elevation bins; therefore, we added the standard deviation of dh for each bin, weighting by the number of points that were filled in that bin. Then we divide by the total number of pixels so that the uncertainty is only accounted for on the fraction of the glacier that is filled. (denoted σ_{fill}) • Uncertainty of radar penetration adjustment: We assume an uncertainty of 1 m for C-band penetration and 4 m for X-band penetration, applied only to non-debris-covered portions of the glacier. (denoted σ_{pen}) • Uncertainty of seasonal adjustment; We used the conservative estimate that the standard deviation is equal to 100% of the magnitude of the adjustment made. (denoted σ_{seas}) • Uncertainty of glacier area: We assumed the standard deviation is half the observed difference between the area calculated using the provided extent (809 km²) and the area calculated from the TanDEM-X DEM (843 km²), or about 20 km². (denoted σ_S, for surface area) <p>The standard error of mean elevation change is $\sigma_{dh} = \sqrt{(\sigma_{dz}^2 + \sigma_{fill}^2 + \sigma_{pen}^2 + \sigma_{seas}^2)/N_{eff}}$</p> <p>The standard error of volume change is $\sigma_{dV} = \sqrt{(\sigma_{dh}^2 * S^2 + dh^2 * \sigma_S^2 + \sigma_{dh}^2 * \sigma_S^2)}$</p> <p>Where S is the surface area of the glacier. Note that the usual propagation of error equation for a product ($dh * S$) would omit the last term ($\sigma_{dh}^2 * \sigma_S^2$) under the assumption that this value is small; however, we chose to include it here as it is more exact.</p>

Table S9. LEG spaceborne results.

GROUP NAME	LEG – LEGOS, Laboratoire d'Etudes en Géophysique et Océanographie Spatiales	
AUTHORS and AFFILIATIONS	Etienne Berthier¹ ¹ Université de Toulouse, LEGOS (CNES/CNRS/IRD/UPS), Toulouse, France	
GLACIER	Hintereisferner (HEF), Grosser Aletschgletscher (ALE), Baltoro (BAL)	
GROUP-#	LEG-1	
QUALITY FLAG	—	
SOURCE	ASTER	
DEM	Provided DEMs	
PROCESSING (dh)	DEM difference	
REFERENCE DEM	For HEF and ALE: Oldest of the two compared ASTER DEMs	BAL Copernicus DEM
COREGISTRATION	Berthier et al., 2007	
BIAS	Correction for the across and along track shifts inspired by Gardelle et al. (2013) improved by fitting a spline to the residuals along track.	
FILTERING	Values outside ± 10 m/yr are filtered out in the final dh/dt map and considered as data void. To compute the glacier-wide average, in each altitude band, values outside 3 standard deviation of the mean elevation difference are filtered out	

VOID-FILLING	A local hypsometric method, as defined by (McNabb et al., 2019), using 100 m elevation intervals
RADAR PENETRATION	Not applicable
TEMPORAL	To take into account the missing (Aletsch) or excess (Hintereisferner) year, the glacier-wide mean elevation during this year was corrected using the regional mass balance anomaly of Central Europe taken from (Zemp et al., 2019, 2010)
UNCERTAINTY (dh_sigma)	The total uncertainty is computed by considering four sources of uncertainties: <ul style="list-style-type: none"> the elevation changes for measured pixels, quantified using the patch method as described in the supplement of Wagnon et al. (2021). the elevation changed for unmeasured pixels, using a factor 5 from Berthier et al. (2014) the inventory, assuming a 10% error at the 95 CI (the 5% value from Paul et al. (2013) multiplied by two). the “temporal” correction, i.e., our measurement period misses one full year for Aletsch (or includes an additional year for Hintereisferner).

Table S10. LMI spaceborne results.

GROUP NAME	LMI – National Land Survey of Iceland
AUTHORs and AFFILIATIONs	Joaquín M.C. Belart^{1,2} ¹ National Land Survey of Iceland, Akranes, Iceland ² Institute of Earth Sciences, University of Iceland, Reykjavík, Iceland
GLACIER	Hintereisferner, Grosser Aletschgletscher
GROUP-#	LMI-1
QUALITY FLAG	—
SOURCE	ASTER
DEM	Provided DEM time series
PROCESSING (dh)	The generation of the dh map was done using the steps described in Hugonnet et al. (2021), specifically: 1) DEM co-registration, 2) DEM stacking, 3) DEM filtering and 4) spatiotemporal homogenisation using Gaussian Process regression. The processing was done with the original spatial resolution of the DEMs (30x30 m) and with a time interval for temporal interpolation of 15 days. Volume changes were obtained from the average dh of the glacier, multiplied by the glacier area.
REFERENCE DEM	Copernicus DEM
COREGISTRATION	Nuth and Kääb (2011); Shean et al. (2016)
BIAS	Not applicable
FILTERING	The stack of ASTER DEMs was filtered using the spatial filter from Hugonnet et al. (2021), equation S1.
VOID-FILLING	The Gaussian Process regression yielded a stack of spatially-filled synthetic DEMs; therefore, no gap-filling was needed for the processing.
RADAR PENETRATION	Not applicable
TEMPORAL	The Gaussian Process regression yielded a stack of synthetic DEMs every 15 days. The closest DEMs to the desired time period were: <ul style="list-style-type: none"> Alesch: 16 September 2011 and 16 September 2017 Hintereisferner: 2 October 2010 and 17 September 2019 No further temporal corrections were done in this test
UNCERTAINTY	The uncertainties (95% confidence interval) of the volume change were estimated using the methods described in Magnússon et al. (2016).

Table S11. UGA spaceborne results.

GROUP NAME	UGA – Université Grenoble Alpes			
AUTHORs and AFFILIATIONS	Amaury Dehecq¹, Friedrich Knuth², Shashank Bhushan², David Shean², Erik Mannerfelt^{3,4}, Romain Hugonnet^{3,4,5} ¹ Univ. Grenoble Alpes, IRD, CNRS, INRAE, Grenoble INP, IGE, 38000 Grenoble, France ² University of Washington, Department of Civil and Environmental Engineering, Seattle, WA, USA ³ Laboratory of Hydraulics, Hydrology and Glaciology (VAW), ETH Zurich, Zurich, Switzerland. ⁴ Swiss Federal Institute for Forest, Snow and Landscape Research (WSL), Birmensdorf, Switzerland. ⁵ Centre d'Etudes Spatiales de la Biosphère, CESBIO, Univ. Toulouse, CNES/CNRS/INRA/IRD/UPS, 31401 Toulouse, France.			
GLACIER	Hintereisferner, Grosser Aletschgletscher, Vestisen, Baltoro, Northern Patagonian Icefield			
GROUP-#	UGA-1	UGA-2	UGA-3	UGA-4
QUALITY FLAG	Low confidence for VES, BAL, and NPI due to insufficient coverage for the automatic (experimental) DEM selection.	Low confidence for VES, BAL, and NPI due to insufficient coverage for the automatic (experimental) DEM selection.	—	—
SOURCE	ASTER			
DEM	Provided DEMs			
PROCESSING (dh)	<ul style="list-style-type: none"> Select DEMs within ± 400 days around validation dates and selected months (Aug, Sep, Oct) Keep DEM with the best coverage over ROI for each validation date (no mosaicking) DEM difference 	<ul style="list-style-type: none"> Select DEMs within ± 400 days around validation dates and selected months (Aug, Sep, Oct) Calculate the median of all DEMs for each validation date DEM difference 	<ul style="list-style-type: none"> Select all DEMs between the validation dates + 365 days at each end. Theil-Sen regression 	<ul style="list-style-type: none"> Select all DEMs Theil-Sen regression
REFERENCE DEM	Provided Copernicus DEM			
COREGISTRATION	The scripts to calculate glacier mass balance as part of the IACS RAGMAC are available at https://github.com/adehecq/ragmac_xdem . Correct horizontal shift using Nuth and Kääb (2011) algorithm (xdem implementation, https://xdem.readthedocs.io/) We use pixels outside RGI outlines, with slope < 50 degree and elevation diff < 5 NMAD of all off-glacier pixels.			
BIAS	In addition to co-registration, we applied the following bias corrections: <ul style="list-style-type: none"> remove degree 1 spatial polynomial vertical bias remove median vertical bias. 			
FILTERING	Spatial filter from Hugonnet et al. (2021), equation S1. In brief, we exclude pixels for which the absolute elevation difference to the maximum or minimum reference elevation found within a disk D of radius r was larger than a vertical elevation threshold Δh . This is done sequentially for three sets of r and Δh values: (200, 700), (500, 500), (1000, 300).			
	—	—	During temporal regression, pixels with less than 5 observations or with time separation between the first and last dates less than 50% of the validation period or 4 years, are excluded.	
VOID-FILLING	Regional hypsometric approach: i) We group all pixels of all glaciers in the ROI into 100 m elevation bins.			

	ii) We calculate the median elevation change of all pixels in each bin. We exclude pixels with a slope > 45 degrees. iii) Bins with less than 10 observations are excluded. iv) Missing bins are filled using a linear interpolation. In case of missing bins on the edges, the nearest value is used. v) All pixels with non-valid observations are replaced by the median value of their corresponding elevation bin.	
RADAR PENETRATION	Not applicable	
TEMPORAL	—	Elevation change rate (dh/dt) was calculated during regression, and then elevation change (dh) was calculated exactly for the validation period.
UNCERTAINTY (dh_sigma)	We account for uncertainties in a) the mean elevation changes $\sigma_{<\Delta h>}$ b) area uncertainties σ_A c) uncertainties related to the interpolation of missing values σ_{interp} . Each uncertainty is detailed below. a) We calculate the standard error of the mean, assuming a spatial correlation length of errors of 500 m, following the method of Rolstad et al. (2009) and as implemented in xDEM. b) Calculated in a way similar to Hugonnet et al. (2021), i.e. a buffer of 30 m is added around the RGI outlines. The relative error in the area is calculated as $\sigma_A = (A_{\text{RGI}+30} - A_{\text{RGI}}) / A_{\text{RGI}}$. c) The uncertainty for missing values is considered as 5 times the uncertainty of measured pixels, as in Berthier et al. (2014). We call p the proportion of measured pixels. The final uncertainty in volume change is calculated as $\sigma_{\Delta V} = \text{sqrt}(\sigma_{<\Delta h>}(p + 5(1 - p))A)^2 + (\sigma_A <\Delta h >)^2$ All reported errors are provided as 2-sigma.	

Table S12. UIO spaceborne results.

GROUP NAME	UIO – University of Oslo				
AUTHORs and AFFILIATIONs	Livia Piermattei^{1,2}, Désirée Treichler², Ruitang Yang², Luc Girod², Robert McNabb³, Andreas Käab² ¹ Department of Land Change Science, Swiss Federal Institute for Forest, Snow and Landscape Research WSL, Birmensdorf, Switzerland ² Department of Geosciences, University of Oslo, Oslo, Norway ³ School of Geography and Environmental Sciences, Ulster University, Coleraine, UK				
GLACIER	Hintereisferner				
GROUP-#	UIO-1	UIO-2	UIO-3	UIO-4	UIO-5
QUALITY FLAG	—	—	—	—	Low confidence: <ul style="list-style-type: none"> • Unrealistic (i.e. large positive) mean elevation change along the all-orographic right of the glacier tongue. • Elevation change rate over 7 years (0.51 m/yr) is too small for an alpine glacier.
SOURCE	ASTER, TanDEM-X	ASTER, TanDEM-X	ASTER	ASTER	
DEM	Provided pair DEMs			Provided DEMs time series (only summer months, July-October)	
PROCESSING (dh)	DEM differencing (DEMdiff)			Median elevation within fixed elevation bands (100 m)	
				Linear interpolation	RANSAC linear interpolation
REFERENCE DEM	Copernicus DEM as reference for co-registration				
COREGISTRATION	Full 3D affine transformation parameters (OpalsLSM, Pfeifer et al., 2014) on stable terrain defined as off-RGI			Nuth and Käab (2011) on stable terrain defined as off-RGI area	

	area, excluding cells with slope values greater than 40°		
BIAS	—		
FILTERING	5x5 median filter of the DEMdiff. Outliers = pixels where the abs. difference between the DEMdiff and the median DEMdiff > the std of their differences		Outlier = DEMdiff between the ASTER DEM and the reference DEM > 100 m
VOID-FILLING	hypsoetry of DEMdiff (mean, elevation bin 50 m)	IDW of DEMdiff	—
RADAR PENETRATION	Not applicable		
TEMPORAL	—	annual correction using WGMS data	annual correction using WGMS data
UNCERTAINTY	One NMAD of the elevation change off-glacier		The area-weighted mean of the RMSE of the residuals between the measured elevation (i.e. from the DEM) and the predicted elevation by the regression. The uncertainty of the DEM is not considered

GROUP NAME	UIO – University of Oslo						
AUTHORS and AFFILIATIONS	Livia Piermattei^{1,2}, Désirée Treichler², Ruitang Yang², Luc Girod², Robert McNabb³, Andreas Kääh² 1 Department of Land Change Science, Swiss Federal Institute for Forest, Snow and Landscape Research WSL, Birmensdorf, Switzerland 2 Department of Geosciences, University of Oslo, Oslo, Norway 3 School of Geography and Environmental Sciences, Ulster University, Coleraine, UK						
GLACIER	Vestisen						
GROUP-#	UIO-1	UIO-2	UIO-3	UIO-4	UIO-5	RUIO-6	UIO-7
QUALITY FLAG	Low confidence: Due to extensive data voids and very few cells in certain elevation bands, massive interpolation is required. Thus, it is difficult to assess the accuracy of the glacier elevation change, even considering the glacier complex for hypsometric interpolation (Fig. A6, labelled UIO-1 & UIO-2).		Low confidence: Due to extensive data voids and remaining noise, the IDW interpolation provided an unrealistic glacier elevation change pattern (Fig. A6, labelled as UIO-3).	Low confidence: The RANSAC linear interpolation applied to the time series for individual glaciers yielded elevation changes exhibiting unrealistic patterns, such as opposite values on the same elevation band for the neighbouring glaciers (Fig. A6, labelled UIO-4).	—	—	—
SOURCE	ASTER						
DEM	Provided pair DEMs			Provided DEMs time series (only summer months, July-October)		Processed pair DEMs	
PROCESSING (dh)	DEM differencing (DEMdiff)			Median elevation within fixed elevation bands (100 m)		ASTER images processed with MMASTER	

		individual glacier	glacier complex	
		RANSAC linear interpolation		
REFERENCE DEM	Copernicus DEM as reference for co-registration			
COREGISTRATION	Full 3D affine transformation parameters (OpalsLSM, Pfeifer et al. 2014) on stable terrain defined as the off-RGI area, excluding cells with slope values greater than 40 degrees	Nuth and Kääb (2011) on stable terrain defined as off-RGI area		Nuth and Kääb (2011) OpalsLSM
BIAS	—			Remove satellite jitter
FILTERING	5x5 median filter of the DEMdiff. Outliers = pixels where the abs. difference between the DEMdiff and the median DEMdiff > the std of their differences	Outlier = DEMdiff between the ASTER DEM and the reference DEM > 100 m		—
VOID FILLING	hypsometry of DEMdiff (mean elevation bin 50 m)	IDW of DEMdiff (glacier complex)	—	Hypsometry of DEMdiff (mean elevation bin 50 m) glacier complex
	individual glacier	glacier complex		
RADAR PENETRATION	Not applicable			
TEMPORAL	—			
UNCERTAINTY	One NMAD of the elevation change off-glacier	Area-weighted mean of the RMSE of the residuals between the measured elevation (i.e. from the DEM) and the predicted elevation by the regression. The uncertainty of the DEM is not considered		—

Table S13. USG spaceborne results.

GROUP	USG – United States Geological Survey			
AUTHORS and AFFILIATIONS	Christopher McNeil ¹ , Caitlyn Florentine ² , Louis Sass ¹ ¹ US Geological Survey Alaska Science Center, Anchorage, AK, USA ² US Geological Survey Northern Rocky Mountain Science Center, West Glacier MT, USA			
GLACIER	Hintereisferner	Grosser Aletschgletscher	Vestisen	Baltoro
GROUP-#	USG-1	USG-1	USG-1	USG-1
QUALITY FLAG	—	Low confidence: This result is flagged as low confidence due to the mixed-use of TanDEM-X and ASTER elevation data.	—	—
SOURCE	ASTER	TanDEM-X /ASTER	TanDEM-X	ASTER
DEM	Provided pair DEMs			
PROCESSING (dh)	DEM differencing was performed on a pixel-to-pixel basis, using a bilinear interpolation to resample each selected, co-registered DEM (ASTER or TanDEM-X) to the greater (coarser) resolution of the reference Copernicus DEM.			
REFERENCE DEM	Copernicus DEM as reference for co-registration			

COREGISTRATION	Co-registration was executed using methods described by Nuth and Kääb (2011) and automated by Shean et al. (2016) via the demcoreg tool to minimise elevation differences between DEMs across stable terrain. Stable terrain was automatically selected using the Copernicus Global Land Cover dataset (Buchhorn et al., 2020) and the Randolph Glacier Inventory (RGI Consortium, 2017) to mask out heavily vegetated and glacierised areas. Stable co-registration areas were restricted to areas with slope < 40°. Each DEM was iteratively shifted to minimise residual differences from the reference DEM (Nuth and Kääb, 2011) until the applied shifts in the northing, easting, and vertical dimensions reached the minimum tolerance of 0.1 m.
BIAS	—
FILTERING	—
VOID-FILLING	Gap filling was performed on DEMs with < 95% glacier coverage using the ‘Local Hypsometry – Mean elevation difference by elevation bin’ method (McNabb et al., 2019).
RADAR PENETRATION	Not applicable
TEMPORAL	—
UNCERTAINTY (dh_sigma)	<p>Glacier area error was calculated using the RGI inverse power law uncertainty function described by (Pfeffer and others, 2014) for the designated RGI glacier(s) for each site. Glacier elevation change errors reflect the area-weighted average of Normalized Median Absolute Deviation (NMAD) and the Mean Absolute Error (MAE) of observed vs predicted values from the specific interpolation function applied to each glacier (Höhle and Höhle, 2009; McNeil et al., 2020; O’Neel et al., 2019).</p> <p>The NMAD reflects random elevation error of any pixel across the DEM-differenced elevation change grid (Shean et al., 2016). The MAE reflects the error of any interpolated elevation value, i.e. void fill. These two elevation uncertainty components were weighted by the fraction of the glacier area covered by the DEM:</p> $dh\sigma = NMAD(1-f) + (MAE + NMAD)f$ <p>where f is the fraction of the glacier area that required interpolation and $1-f$ is the fraction of the glacier area that did not require interpolation. The total combined elevation change error ($dh\sigma$) was calculated for each individual DEM and then summed in quadrature for DEM differences. The void fill error provided in error results is the $(MAE + NMAD)f$ term of this equation.</p> <p>For glaciers with > 95% data coverage, no interpolation was applied. Accordingly, the NMAD represents 100% of the uncertainty in mean elevation change for DEM differences where less than 5% of the glacier area was missing. Uncertainties in glacier volume change were calculated by summing area and elevation change errors in quadrature.</p>

Table S14. UST spaceborne results.

GROUP NAME	UST – University of St. Andrews							
AUTHORs and AFFILIATIONs	Tobias Bolch^{1,2}, Gregoire Guillet^{1,3,4}, Atanu Bhattacharya^{1,5}, Daniel Falaschi^{1,6}, Owen King¹, Sajid Ghuffar^{1,7} ¹ School of Geography and Sustainable Development, University of St Andrews, Scotland, UK ² Institute of Geodesy, Graz University of Technology, Graz, Austria ³ Civil and Environmental Engineering, University of Washington, Seattle, WA, USA ⁴ Department of Geosciences, University of Oslo, Oslo, 0371, Norway ⁵ Department of Earth Sciences and Remote Sensing, JIS University, Kolkata, India ⁶ Instituto Argentino de Nivología, Glaciología y Ciencias Ambientales (IANIGLA), Mendoza, Argentina ⁷ Department of Space Science, Institute of Space Technology, Islamabad, Pakistan							
GLACIER	Baltoro				Northern Patagonian Icefield			
GROUP-#	UST-1	UST-2	UST-3	UST-4	UST-1	UST-2	UST-3	UST-4
QUALITY FLAG	—	—	—	—	—	—	—	—
SOURCE	SRTM/ASTER; ASTER/ASTER				SRTM/ASTER; ASTER/TanDEM-X			
DEM	Provided DEMs							
PROCESSING (dh)	DEM differencing was performed on a pixel-to-pixel basis							

REFERENCE DEM	Copernicus DEM as reference for co-registration		
COREGISTRATION	Nuth and Kääb (2011) on stable terrain, the tilt between two DEMs was estimated using Pieczonka et al. 2013, small rotational effects and de-ramping were eliminated using Pieczonka and Bolch (2015)		
BIAS	—		
FILTERING	Surface elevation change estimates (ΔH) are inferred probabilistically from the observed elevation changes and the physical knowledge we have of glaciers in general (Guillet and Bolch, 2023)	Absolute elevation differences of ± 150 m were removed. The remaining outliers were removed as proposed by (Gardelle et al. 2013)	Absolute elevation differences of ± 150 m were removed. The remaining outliers were removed as proposed by Pieczonka and Bolch (2015)
VOID-FILLING	Void-filling approach follows the methodology proposed by Guillet and Bolch (2023)	Small data void (< 5 pixels): filled by the mean elevation of the neighbouring pixels (4×4 pixels windows). 2. Larger data gaps: Global mean hypsometric (McNabb et al. 2019) in 100 m elevation bins	
PENETRATION	Penetration correction is here modelled as an elevation-dependent Gaussian probability distribution as proposed by Agarwal et al. (2017)	No Penetration correction	
TEMPORAL	—		
UNCERTAINTY (Δh_{σ})	Outlier culling and uncertainty quantification are unified within a statistically consistent Bayesian framework proposed by Guillet and Bolch (2023). In brief, glacier surface elevation changes are computed as the median of the posterior probability density through Bayes' theorem ($\text{Posterior} \propto \text{Prior} * \text{Likelihood}$). We use a combination of empirical and modelled priors to define a set of elevation-dependent surface elevation change distributions. In practice, this set of admissible values is represented for each elevation change pixel as a Student-T distribution, where the median of the distribution is defined using the datasets of Shean et al. (2020) and Hugonnet et al. (2021). The distribution scale is computed through modelling and depends on the glacier's ELA. This is to allow for weaker priors near the glacier terminus, ensuring that dynamical instabilities such as surges are correctly captured. The likelihood captures data-related uncertainties. Here, we model pixel-wise uncertainties resulting from terrain roughness, obscured and low-contrast surfaces and penetration of radar beams into snow/ice. Each of these components is modelled independently as a marginal probability distribution. The likelihood is then computed by summing over all the possible events, i.e. the sum of all marginal probabilities. The final uncertainty for each pixel is the spread of the posterior distribution. Note, however, that frequentist and Bayesian uncertainties differ in philosophy and cannot be compared directly. If single-value estimates are preferred, then the median of the (pixel-wise) posterior probability density is a satisfactory estimate, and the spread of the (pixel-wise) distribution of medians over the considered region can be compared to other uncertainty estimates.	The uncertainty associated with the volumetric change was calculated as the quadratic sum of the volumetric uncertainties on mean elevation and glacier area change. The uncertainty estimation on the mean elevation change was calculated using the patch (in various sizes) method (Berthier et al., 2016). To constrain the decay of the error with the averaging area (Wagnon et al., 2021).	

Table S15. UZH spaceborne results.

GROUP	UZH – University of Zurich			
AUTHORs and AFFILIATIONS	Ines Dussaillant ¹ and Michael Zemp ¹ ¹ Department of Geography, University of Zurich, Switzerland			
GLACIER	Hintereisferner, Grosser Aletschgletscher			
GROUP-#	UZH-1	UZH-2	UZH-3	UZH-4
QUALITY FLAG	—	—	—	—
SOURCE	ASTER			
DEM	All Provided DEMs	Provided DEMs from 2011 to 2018	All Provided DEMs	Provided DEMs from 2010 to 2020
PROCESSING (dh)	<ul style="list-style-type: none"> • ASTERiX method as in Dussaillant et al. (2019) • Calibration of regional glacier mass balance anomaly (i.e. temporal variability) from Central Europe glaciological sample to produce an annual glacier mass balance time series. 		<ul style="list-style-type: none"> • ASTERiX method as in Dussaillant et al. (2019) • Calibration of Hintereis glacier mass balance anomaly to produce an annual glacier mass balance time series. 	
REFERENCE DEM	Copernicus DEM			
COREGISTRATION	Horizontal and vertical co-registration from Nuth and Kääb (2011)			
BIAS	Correction for the across and along track shift inspired by Gardelle et al. (2013) improved by fitting a spline to the residuals along track.			
FILTERING	The mean dh/dt rate was computed after excluding: Values lying further than 3-NMAD from the median of the elevation band, <ul style="list-style-type: none"> • Pixels on slopes larger than 45°, (c) pixels with uncertainties in the linear fit larger than 2 m yr⁻¹ (at the 95% confidence level) and (d) absolute dh/dt values larger than 30 m yr⁻¹ 			
VOID-FILLING	Local hypsometric method using 100 m elevation bands (McNabb et al., 2019).			
RADAR PENETRATION	Not applicable			
TEMPORAL	Aletsch has no glaciological observations. Here, we use the regional annual anomaly, which is obtained as the mean of all individual glacier anomalies of the glaciological observation sample for Central Europe. Anomalies are calculated using the period 2009–2018 as a reference. The regional annual anomaly is then calibrated based on the geodetic estimate obtained for each result. Finally, the experiment targeted period for Aletsch glacier is extracted from the annual time series.		The annual glacier change anomaly comes from the in-situ HEF-glaciological observations. Anomalies are calculated using the period 2009–2018 as a reference. The glacier annual anomaly is then calibrated based on the geodetic estimate obtained from each result. Finally, the experiment targeted period for Hintereisferner glacier is extracted from the annual time series.	
UNCERTAINTY (dh_sigma)	Volume change uncertainties were assessed as random errors coming from two main sources, assumed to be independent of one another: <ul style="list-style-type: none"> • The uncertainty in the rate of elevation change (multiplied by a factor of 5 over data voids). • The uncertainty in the glacierised area. Errors are combined according to Rolstad et al. (2009) and Fischer et al. (2015). The calibrated series uncertainty results as the combination of two independent errors: <ul style="list-style-type: none"> • The uncertainty related to the multi-annual geodetic mass change rate (obtained from the main results). • The glacier/regional anomaly uncertainty. The uncertainty of the regional anomaly is calculated as the combination of the mean uncertainty from the glaciological sample and the variability of the individual glacier anomalies at a 95% confidence interval. All these errors are combined according to the law of random error propagation. The methodology is inspired by previous work from Zemp et al. (2019, 2020) and further developed by Dussaillant et al. (2023).			

Table S16. Experiment and validation results for Hintereis (HEF) for the target period from 2010 to 2019.

For each group and run, a summary of data and workflow (0: no; 1: yes) is provided together with survey dates (DD.MM.YYYY) and corresponding elevation changes (dh) in metre.

T0 refers to survey periods without temporal corrections; T1 refers to survey periods with temporal corrections but different from validation period; T2 refers to the validation period.

Final results of all runs are given in dh_T2_final, including temporal corrections to the validation period, if needed. Uncertainties are reported in metre and at 95% confidence levels. Results reported as low confidence have a quality flag of 0

GLACIER	GROUP	RUN	SOURCE	DEM_COUNT	PROVIDED	PROCESSED	PAIR	MOSAIC	TIMESERIES	CO-REGISTRATION	BIAS	NOISE_FILTERING	VOID_FILLING	PENETRATION	TEMPORAL	T0_START	T0_END	T1_START	T1_END	T2_START	T2_END	dh_T0	dh_T1	dh_T2_final	dh_UNCERTAINTY	QUALITY_FLAG
HEF	LMI	1	ASTER	189	1	0	0	0	1	1	0	1	1	0	1			02.10.2010	17.09.2019			-10.711	-10.729	-10.729	0.27	1
HEF	LEG	1	ASTER	2	1	0	1	0	0	1	1	1	1	0	0	03.10.2009	29.09.2019	03.10.2010	29.09.2019			-12.8	-12.111	-12.066	3.46	1
HEF	UGA	1	ASTER	2	1	0	1	0	0	1	1	1	1	0	0	03.10.2009	15.09.2020					-11.212	-9.26	-9.26	1.578	1
HEF	UGA	2	ASTER	22	1	0	0	1	0	1	1	1	1	0	0	26.08.2010	20.09.2019					-8.998	-8.534	-8.534	1.265	1
HEF	UGA	3	ASTER	61	1	0	0	0	1	1	1	1	1	0	1					08.10.2010	21.09.2019		-12.556	-12.556	1.65	1
HEF	UGA	4	ASTER	189	1	0	0	0	1	1	1	1	1	0	1					08.10.2010	21.09.2019		-13.261	-13.261	1.659	1
HEF	UZH	1	ASTER	20	1	0	0	0	1	1	0	1	1	0	0	19.11.2001	22.04.2021	01.10.2010	30.09.2019			-27.21	-13.042	-12.99	0.613	1
HEF	UZH	2	ASTER	14	1	0	0	0	1	1	0	1	1	0	0	27.03.2012	23.09.2019	01.10.2010	30.09.2019			-12.2	-13.984	-13.932	0.747	1
HEF	USG	1	ASTER	2	1	0	1	0	0	1	0	0	1	0	0	27.08.2010	21.09.2019					-9.22	-8.771	-8.771	9.192	1
HEF	ETH	1	ASTER		0	1	0	0	1	1	1	1	1	0	2			01.10.2010	01.10.2019				-12.438	-12.386	4.639	1
HEF	DLR	1	TDX	2	0	1	1	0	0	1	1	1	1	0	1	24.09.2011	11.09.2020			08.10.2010	21.09.2019	-5.14	-5.13	-5.13	2.539	0
HEF	DLR	2	TDX	2	0	1	1	0	0	1	1	1	1	0	1	24.09.2011	09.02.2019			08.10.2010	21.09.2019	-11.29	-13.7	-13.7	1.07	1
HEF	DLR	3	TDX	2	0	1	1	0	0	1	1	1	1	0	1	24.09.2011	09.02.2019			08.10.2010	21.09.2019	-8.74	-10.61	-10.61	0.816	1
HEF	DLR	4	TDX	2	0	1	1	0	0	1	1	1	1	0	1	24.09.2011	11.09.2020			08.10.2010	21.09.2019	-4.06	-4.058	-4.058	1.042	0
HEF	DLR	5	TDX	2	0	1	1	0	0	1	1	1	1	0	1	24.09.2011	09.02.2019			08.10.2010	21.09.2019	-8.19	-9.938	-9.938	1.014	1
HEF	DLR	6	TDX	2	1	0	1	0	0	1	1	1	1	0	1	24.09.2011	09.02.2019			08.10.2010	21.09.2019	-8.78	-10.657	-10.657	1.051	1
HEF	DLR	7	TDX	2	0	1	1	0	0	1	1	1	1	0	1	24.09.2011	09.02.2019			08.10.2010	21.09.2019	-8.44	-10.246	-10.246	0.859	1
HEF	UIO	1	ASTER	2	1	0	1	0	0	1	0	1	1	0	0	03.10.2009	29.09.2019	01.10.2010	30.09.2019			-11.956	-11.026	-10.974	3.593	1
HEF	UIO	2	ASTER	2	1	0	1	0	0	1	0	1	1	0	0	03.10.2009	29.09.2019	01.10.2010	30.09.2019			-12.086	-11.16	-11.108	3.593	1
HEF	UIO	3	ASTER	75	1	0	0	0	1	1	0	1	0	0	1					08.10.2010	21.09.2019		-10.035	-10.035	3.43	1
HEF	UIO	4	ASTER	75	1	0	0	0	1	1	0	1	0	0	1					08.10.2010	21.09.2019		-11.41	-11.41	2.215	1
HEF	UIO	5	TDX	2	1	0	1	0	0	1	0	1	1	0	0	24.09.2011	11.09.2020					-3.905	-4.409	5.926	0	
HEF	UIO	6	TDX	2	1	0	1	0	0	1	0	1	1	0	0	16.02.2012	06.02.2019	01.10.2010	30.09.2019			-6.556	-9.026	-8.974	1.897	1
HEF	FAU	1	ASTER		1	0	0	1	0	1	1	1	1	0	0	18.08.2010	20.09.2019					-7.791	-7.141	-7.141	1.073	1
HEF	FAU	2	TDX		1	0	0	1	0	1	1	1	1	0	0	04.10.2011	21.10.2019					-6.974	-8.173	-8.173	1.429	1
HEF	BAW	1	TDX	2	1	0	1	0	0	1	1	1	1	0	1	16.02.2012	06.02.2019			08.10.2010	21.09.2019	-7.777	-9.978	-9.978	0.777	1
HEF	VAL	1	airborne	2	1	1	1	0	0	1	0	0	0	0	0					08.10.2010	21.09.2019		-10.614	-10.614	0.255	1

Table S17. Experiment and validation results for Aletsch (ALE) for the target period from 2011 to 2017.

For each group and run, a summary of data and workflow (0: no; 1: yes) is provided together with survey dates (DD.MM.YYYY) and corresponding elevation changes (dh) in metre.

T0 refers to survey periods without temporal corrections; T1 refers to survey periods with temporal corrections but different from validation period; T2 refers to the validation period.

Final results of all runs are given in dh_T2_final, including temporal corrections to the validation period, if needed. Uncertainties are reported in metre and at 95% confidence levels. Results reported as low confidence have a quality flag of 0

GLACIER	GROUP	RUN	SOURCE	DEM_COUNT	PROVIDED	PROCESSED	PAIR	MOSAIC	TIMESERIES	CO-REGISTRATION	BIAS	NOISE_FILTERING	VOID_FILLING	PENETRATION	TEMPORAL	T0_START	T0_END	T1_START	T1_END	T2_START	T2_END	dh_T0	dh_T1	dh_T2	dh_T2_final	dh_UNCERTAINTY	QUALITY_FLAG	
ALE	LMI	1	ASTER	168	1	0	0	0	1	1	0	1	1	0	1			16.09.2011	16.09.2017				-7.423		-7.535	0.18	1	
ALE	LEG	1	ASTER	2	1	0	1	0	0	1	1	1	1	0	1	07.09.2012	05.09.2017	07.09.2011	05.09.2017				-6.9	-9.019	-9.219	2.12	1	
ALE	UGA	1	ASTER	2	1	0	1	0	0	1	1	1	1	0	0	23.09.2012	02.09.2016						-2.605		-6.362	0.455	1	
ALE	UGA	2	ASTER	18	1	0	0	1	0	1	1	1	1	0	0	22.08.2012	25.09.2016						-6.127		-8.914	0.404	1	
ALE	UGA	3	ASTER	39	1	0	0	0	1	1	1	1	1	0	2					13.09.2011	21.09.2017			-9.374	-9.374	0.609	1	
ALE	UGA	4	ASTER	168	1	0	0	0	1	1	1	1	1	0	2					13.09.2011	21.09.2017			-8.061	-8.061	0.484	1	
ALE	UZH	1	ASTER	12	1	0	0	0	1	1	0	1	1	0	1	30.07.2001	22.04.2020	01.10.2011	30.09.2017				-24.697	-9.275	-9.363	2.466	1	
ALE	UZH	2	ASTER	6	1	0	0	0	1	1	0	1	1	0	1	01.06.2012	16.09.2017	01.10.2011	30.09.2017				-6.37	-7.6	-7.688	2.54	1	
ALE	USG	1	ASTER/TDX	2	1	0	1	0	0	1	0	0	1	0	0	23.09.2011	22.09.2017						-2.59		-2.694	15.576	0	
ALE	ETH	1	ASTER		0	1	0	0	1	1	1	1	1	0	2			01.09.2011	01.09.2017					-8.533	-8.711	3.233	1	
ALE	DLR	1	TDX	4	0	1	0	1	0	1	1	1	1	0	1	21.08.2011	03.01.2018			13.09.2011	21.09.2017			-12.88	-12.173	-12.173	0.37	0
ALE	DLR	2	TDX	4	0	1	0	1	0	1	1	1	1	0	1	21.08.2011	03.01.2018			13.09.2011	21.09.2017			-12.14	-11.479	-11.479	0.417	0
ALE	DLR	3	TDX	4	0	1	0	1	0	1	1	1	1	0	1	21.08.2011	03.01.2018			13.09.2011	21.09.2017			-11.5	-10.868	-10.868	0.301	0
ALE	DLR	4	TDX	4	0	1	0	1	0	1	1	1	1	0	1	21.08.2011	03.01.2018			13.09.2011	21.09.2017			-10.83	-10.239	-10.239	0.396	0
ALE	DLR	5	TDX	4	1	0	0	1	0	1	1	1	1	0	1	21.08.2011	03.01.2018			13.09.2011	21.09.2017			-11.83	-11.186	-11.186	0.134	0
ALE	DLR	6	TDX	2	1	0	1	0	0	1	1	1	1	0	1	21.03.2013	01.01.2019			13.09.2011	21.09.2017			-7.25	-7.547	-7.547	0.117	1
ALE	FAU	1	ASTER		1	0	0	1	0	1	1	1	1	0	0	21.03.2011	16.09.2018						-10.993		-7.683	0.679	1	
ALE	FAU	2	TDX		1	0	0	1	0	1	1	1	1	0	0	19.01.2012	12.12.2017						-8.854		-8.624	0.547	1	
ALE	BAW	1	TDX	2	1	0	1	0	0	1	1	1	1	0	1	21.03.2013	01.01.2019			13.09.2011	21.09.2017			-6.987	-7.276	-7.276	0.945	1
ALE	VAL	1	airborne	2	1	1	1	0	0	0	0	0	0	0	0					13.09.2011	21.09.2017			-6.88	-6.88	0.921	1	

Table S18. Experiment and validation results for Vestisen (VES) for the target period from 2008 to 2020.

For each group and run, a summary of data and workflow (0: no; 1: yes) is provided together with survey dates (DD.MM.YYYY) and corresponding elevation changes (dh) in metre

T0 refers to survey periods without temporal corrections; T1 refers to survey periods with temporal corrections but different from validation period; T2 refers to the validation period

Final results of all runs are given in dh_T2_final, including temporal corrections to the validation period, if needed. Uncertainties are reported in metre and at 95% confidence levels. Results reported as low confidence have a quality flag of 0

GLACIER	GROUP	RUN	SOURCE	DEM_COUNT	PROVIDED	PROCESSED	PAIR	MOSAIC	TIMESERIES	CO-REGISTRATION	BIAS	NOISE_FILTERING	VOID_FILLING	PENETRATION	TEMPORAL	T0_START	T0_END	T1_START	T1_END	T2_START	T2_END	dh_T0	dh_T1	dh_T2	dh_T2_final	dh_UNCERTAINTY	QUALITY_FLAG	
VES	UGA	2	ASTER	2	1	0	0	1	0	1	1	1	1	0	0	08.08.2009	25.08.2021								-18.3	-16.818	3.53	0
VES	UGA	3	ASTER	30	1	0	0	0	1	1	1	1	1	0	2					02.09.2008	10.08.2020				14.58	14.58	3.06	0
VES	UGA	4	ASTER	79	1	0	0	0	1	1	1	1	1	0	2					02.09.2008	10.08.2020				-9.65	-9.65	1.06	1
VES	USG	1	TDX	2	1	0	1	0	0	1	0	0	1	0	0	20.03.2011	01.01.2021								-1.43	-0.776	2.89	1
VES	ETH	1	ASTER	0	1	0	0	0	1	1	1	1	1	0	0	01.09.2007	01.08.2019								-5.54	-4.756	4.13	1
VES	UIO	1	ASTER	2	1	0	1	0	0	1	0	1	1	0	0	11.08.2006	28.07.2019								0.24	1.366	3.86	0
VES	UIO	2	ASTER	2	1	0	1	0	0	1	0	1	1	0	0	11.08.2006	28.07.2019								-1.12	0.006	3.86	0
VES	UIO	3	ASTER	2	1	0	1	0	0	1	0	1	1	0	0	11.08.2006	28.07.2019								-0.42	0.706	5.35	0
VES	UIO	4	ASTER	82	1	0	0	0	1	1	0	1	0	0	2					02.09.2008	10.08.2020				-2.71	-2.71	5.88	0
VES	UIO	5	ASTER	82	1	0	0	0	1	1	0	1	0	0	2					02.09.2008	10.08.2020				-2.9	-2.9	4.14	1
VES	UIO	6	ASTER	2	0	1	1	0	0	1	1	1	1	0	0	11.08.2006	28.07.2019								-5.01	-3.884	4.16	1
VES	UIO	7	ASTER	2	0	1	1	0	0	1	1	1	1	0	0	11.08.2006	28.07.2019								-3.47	-2.344	3.86	1
VES	FAU	1	ASTER	1	1	0	0	1	0	1	1	1	1	0	0	01.06.2007	26.08.2021								18.56	22.013	1.2	0
VES	FAU	2	TDX	1	1	0	0	1	0	1	1	1	1	0	0	20.03.2011	01.01.2021								-1.82	-1.166	0.19	1
VES	VAL	1	airborne	2	1	1	1	0	0	1	0	0	0	0	0					02.09.2008	10.08.2020				-4.26	-4.26	0.18	1

Table S19. Experiment results for Baltoro (BAL) for the target period from 2000 to 2012.

For each group and run, a summary of data and workflow (0: no; 1: yes) is provided together with survey dates (DD.MM.YYYY) and corresponding elevation changes (dh) in metre. Uncertainties are reported in metre and at 95% confidence levels. Results reported as low confidence as well as sensitivity runs (e.g., NO-CO: no co-registration) have a quality flag of 0. Start and end dates of the target period (TAR) are given in the last row.

GLACIER	GROUP	RUN	RUN_NAME	SOURCE	DEM_COUNT	PROVIDED	PROCESSED	PAIR	MOSAIC	TIMESERIES	CO-REGISTRATION	BIAS	NOISE_FILTERING	VOID_FILLING	PENETRATION	TEMPORAL	START_DATE	END_DATE	dh	dh_UNCERTAINTY	QUALITY_FLAG
BAL	LEG	1	CTL	ASTER/ASTER	4	1	0	0	1	0	1	1	1	1	0	0	01.02.2000	01.10.2012	2.647	7.77	1
BAL	LEG	1	NO-BIAS	ASTER/ASTER	4	1	0	0	1	0	1	0	1	1	0	0	01.02.2000	01.10.2012	1.489	11.13	0
BAL	LEG	1	NO-CO	ASTER/ASTER	4	1	0	0	1	0	0	1	1	1	0	0	01.02.2000	01.10.2012	1.017	23.72	0
BAL	UST	1	CTL	SRTM/ASTER	2	1	0	1	0	0	1	1	1	1	1	0	16.02.2000	20.08.2012	-1.79	3.83	1
BAL	UST	1	NO-CO	SRTM/ASTER	2	1	0	1	0	0	0	0	1	1	1	0	16.02.2000	20.08.2012	-2.65	3.85	0
BAL	UST	1	NO-GAP	SRTM/ASTER	2	1	0	1	0	0	1	1	0	0	1	0	16.02.2000	20.08.2012	-0.727	4.1	0
BAL	UST	1	NO-PEN	SRTM/ASTER	2	1	0	1	0	0	1	1	1	1	0	0	16.02.2000	20.08.2012	-0.6	3.5	0
BAL	UGA	1	CTL	ASTER/ASTER	2	1	0	1	0	0	1	1	1	1	0	0	11.09.2000	10.10.2013	-2.796	0.579	0
BAL	UGA	2	CTL	ASTER/ASTER	5	1	0	0	1	0	1	1	1	1	0	0	11.09.2000	28.09.2012	-1.784	0.511	0
BAL	UGA	3	CTL	ASTER/ASTER	79	1	0	0	0	1	1	1	1	1	0	1	01.02.2000	01.10.2011	-2.431	0.224	1
BAL	UGA	4	CTL	ASTER/ASTER	119	1	0	0	0	1	1	1	1	1	0	1	01.02.2000	01.10.2011	-0.309	0.059	1
BAL	UGA	1	NO-BIAS	ASTER/ASTER	2	1	0	1	0	0	1	0	1	1	0	0	11.09.2000	10.10.2013	-3.182	0.625	0
BAL	UGA	2	NO-BIAS	ASTER/ASTER	5	1	0	0	1	0	1	0	1	1	0	0	11.09.2000	28.09.2012	-2.926	0.555	0
BAL	UGA	3	NO-BIAS	ASTER/ASTER	79	1	0	0	0	1	1	0	1	1	0	1	01.02.2000	01.10.2011	-0.914	0.151	0
BAL	UGA	1	NO-CO	ASTER/ASTER	2	1	0	1	0	0	0	1	1	1	0	0	11.09.2000	10.10.2013	-17.669	1.821	0
BAL	UGA	2	NO-CO	ASTER/ASTER	5	1	0	0	1	0	0	1	1	1	0	0	11.09.2000	28.09.2012	-12.905	1.533	0
BAL	UGA	3	NO-CO	ASTER/ASTER	79	1	0	0	0	1	0	1	1	1	0	1	01.02.2000	01.10.2011	-19.585	1.513	0
BAL	UGA	1	NO-FIL	ASTER/ASTER	2	1	0	1	0	0	0	1	1	1	0	0	11.09.2000	10.10.2013	-2.978	0.584	0
BAL	UGA	2	NO-FIL	ASTER/ASTER	5	1	0	0	1	0	1	1	0	1	0	0	11.09.2000	28.09.2012	-1.102	0.5	0
BAL	UGA	3	NO-FIL	ASTER/ASTER	79	1	0	0	0	1	1	1	0	1	0	1	01.02.2000	01.10.2011	-2.399	0.222	0
BAL	UGA	1	NO-GAP	ASTER/ASTER	2	1	0	1	0	0	0	1	1	0	0	0	11.09.2000	10.10.2013	-5.474	0.681	0
BAL	UGA	2	NO-GAP	ASTER/ASTER	5	1	0	0	1	0	1	1	1	0	0	0	11.09.2000	28.09.2012	-4.373	0.595	0
BAL	UGA	3	NO-GAP	ASTER/ASTER	79	1	0	0	0	1	1	1	1	0	0	1	01.02.2000	01.10.2011	-2.676	0.24	0
BAL	USG	1	CTL	ASTER/ASTER	2	1	0	1	0	0	0	1	0	0	0	0	28.12.2001	06.05.2011	5.229	15.9	1
BAL	USG	1	NO-CO	ASTER/ASTER	2	1	0	1	0	0	0	0	0	1	0	0	28.12.2001	06.05.2011	2.12	15.6	0
BAL	USG	1	NO-GAP	ASTER/ASTER	2	1	0	1	0	0	1	0	0	0	0	0	28.12.2001	06.05.2011	3.42	11.6	0
BAL	ETH	1	CTL	ASTER/ASTER		0	1	0	0	1	1	1	1	1	0	1	01.02.2000	01.10.2012	-1.055	3.032	1
BAL	GAC	1	CTL	SRTM/TDX	4	1	0	0	1	0	1	1	1	1	1	0	16.02.2000	20.02.2012	0.67	7.2	1
BAL	GAC	1	NO-BIAS	SRTM/TDX	4	1	0	0	1	0	1	0	1	1	1	0	16.02.2000	20.02.2012	-0.07	6.95	0
BAL	GAC	1	NO-CO	SRTM/TDX	4	1	0	0	1	0	0	1	1	1	1	0	16.02.2000	20.02.2012	-3.92	7.94	0
BAL	GAC	1	NO-FIL	SRTM/TDX	4	1	0	0	1	0	1	1	0	1	1	0	16.02.2000	20.02.2012	0.94	9.74	0
BAL	GAC	1	NO-GAP	SRTM/TDX	4	1	0	0	1	0	1	1	0	0	1	0	16.02.2000	20.02.2012	-1.23	7.51	0
BAL	GAC	1	NO-PEN	SRTM/TDX	4	1	0	0	1	0	1	1	1	1	0	0	16.02.2000	20.02.2012	2.72	7.72	0
BAL	FAU	1	CTL	ASTER/ASTER	22	1	0	0	1	0	1	1	1	1	0	0	19.07.2000	28.03.2011	-0.521	0.153	1
BAL	FAU	2	CTL	SRTM/TDX	4	1	0	0	1	0	1	1	1	1	0	0	16.02.2000	09.02.2012	-1.202	0.066	1
BAL	FAU	2	NO-CO	SRTM/TDX	4	1	0	0	1	0	0	1	1	1	0	0	16.02.2000	09.02.2012	-13.014	0.517	0
BAL	FAU	2	NO-FIL	SRTM/TDX	4	1	0	0	1	0	1	1	0	1	0	0	16.02.2000	09.02.2012	-1.142	0.066	0
BAL	FAU	2	NO-GAP	SRTM/TDX	4	1	0	0	1	0	1	1	1	0	0	0	16.02.2000	09.02.2012	-1.655	0.066	0
BAL	TAR	1															01.02.2000	01.10.2012			

Table S20. Experiment results for Baltoro (BAL) for the target period from 2012 to 2019.

For each group and run, a summary of data and workflow (0: no; 1: yes) is provided together with survey dates (DD.MM.YYYY) and corresponding elevation changes (dh) in metre. Uncertainties are reported in metre and at 95% confidence levels. Results reported as low confidence as well as sensitivity runs (e.g., NO-CO: no co-registration) have a quality flag of 0. Start and end dates of the target period (TAR) are given in the last row.

GLACIER	GROUP	RUN	RUN_NAME	SOURCE	DEM_COUNT	PROVIDED	PROCESSED	PAIR	MOSAIC	TIMESERIES	CO-REGISTRATION	BIAS	NOISE_FILTERING	VOID_FILLING	PENETRATION	TEMPORAL	START_DATE	END_DATE	dh	dh_UNCERTAINTY	QUALITY_FLAG
BAL	LEG	1	CTL	ASTER/ASTER	3	1	0	0	1	0	1	1	1	1	0	0	01.10.2012	01.10.2019	-1.889	4.02	1
BAL	LEG	1	NO-BIAS	ASTER/ASTER	3	1	0	0	1	0	1	0	1	1	0	0	01.10.2012	01.10.2019	-0.374	10.41	0
BAL	LEG	1	NO-CO	ASTER/ASTER	3	1	0	0	1	0	0	1	1	1	0	0	01.10.2012	01.10.2019	1.979	23.64	0
BAL	UST	2	CTL	ASTER/ASTER	2	1	0	1	0	0	1	1	1	1	0	0	20.08.2012	11.10.2019	-0.513	2.28	1
BAL	UST	2	NO-CO	ASTER/ASTER	2	1	0	1	0	0	0	0	1	1	0	0	20.08.2012	11.10.2019	0.006	2.53	0
BAL	UST	2	NO-GAP	ASTER/ASTER	2	1	0	1	0	0	1	1	0	0	0	0	20.08.2012	11.10.2019	-0.63	2.6	0
BAL	UGA	1	CTL	ASTER/ASTER	2	1	0	1	0	0	1	1	1	1	0	0	10.10.2013	11.10.2019	-0.366	0.224	0
BAL	UGA	2	CTL	ASTER/ASTER	6	1	0	0	1	0	1	1	1	1	0	0	28.09.2012	10.04.2019	-0.36	0.182	0
BAL	UGA	3	CTL	ASTER/ASTER	45	1	0	0	0	1	1	1	1	1	0	1	01.10.2011	01.10.2019	0.055	0.109	1
BAL	UGA	4	CTL	ASTER/ASTER	119	1	0	0	0	1	1	1	1	1	0	1	01.10.2011	01.10.2019	-0.17	0.033	1
BAL	UGA	1	NO-BIAS	ASTER/ASTER	2	1	0	1	0	0	1	0	1	1	0	0	10.10.2013	11.10.2019	-0.478	0.226	0
BAL	UGA	2	NO-BIAS	ASTER/ASTER	6	1	0	0	1	0	1	0	1	1	0	0	28.09.2012	10.04.2019	-0.064	0.185	0
BAL	UGA	3	NO-BIAS	ASTER/ASTER	45	1	0	0	0	1	1	0	1	1	0	1	01.10.2011	01.10.2019	0.181	0.116	0
BAL	UGA	1	NO-CO	ASTER/ASTER	2	1	0	1	0	0	0	1	1	1	0	0	10.10.2013	11.10.2019	11.964	1.291	0
BAL	UGA	2	NO-CO	ASTER/ASTER	6	1	0	0	1	0	0	1	1	1	0	0	28.09.2012	10.04.2019	6.182	0.712	0
BAL	UGA	3	NO-CO	ASTER/ASTER	45	1	0	0	0	1	0	1	1	1	0	1	01.10.2011	01.10.2019	-2.761	0.311	0
BAL	UGA	1	NO-FIL	ASTER/ASTER	2	1	0	1	0	0	1	1	0	1	0	0	10.10.2013	11.10.2019	-0.505	0.226	0
BAL	UGA	2	NO-FIL	ASTER/ASTER	6	1	0	0	1	0	1	1	0	1	0	0	28.09.2012	10.04.2019	-0.483	0.183	0
BAL	UGA	3	NO-FIL	ASTER/ASTER	45	1	0	0	0	1	1	1	0	1	0	1	01.10.2011	01.10.2019	0.086	0.109	0
BAL	UGA	1	NO-GAP	ASTER/ASTER	2	1	0	1	0	0	1	1	0	0	0	0	10.10.2013	11.10.2019	-0.797	0.231	0
BAL	UGA	2	NO-GAP	ASTER/ASTER	6	1	0	0	1	0	1	1	0	0	0	0	28.09.2012	10.04.2019	-0.758	0.189	0
BAL	UGA	3	NO-GAP	ASTER/ASTER	45	1	0	0	0	1	1	1	0	0	0	1	01.10.2011	01.10.2019	-0.053	0.109	0
BAL	USG	1	CTL	ASTER/ASTER	2	1	0	1	0	0	1	0	0	1	0	0	06.05.2011	12.10.2019	-3.38	15.6	1
BAL	USG	1	NO-CO	ASTER/ASTER	2	1	0	1	0	0	0	0	0	0	0	0	06.05.2011	12.10.2019	0.26	15.7	0
BAL	USG	1	NO-GAP	ASTER/ASTER	2	1	0	1	0	0	1	0	0	0	0	0	06.05.2011	12.10.2019	-3.33	11.7	0
BAL	ETH	1	CTL	ASTER/ASTER	0	0	1	0	0	1	1	1	1	1	0	1	01.10.2012	01.10.2019	-0.037	2.472	1
BAL	GAC	2	CTL	TDX/TDX	6	1	0	0	1	0	1	1	1	1	1	1	20.02.2012	15.01.2020	-3.63	14.05	1
BAL	GAC	2	NO-BIAS	TDX/TDX	6	1	0	0	1	0	1	0	1	1	1	0	20.02.2012	15.01.2020	-0.83	13.85	0
BAL	GAC	2	NO-CO	TDX/TDX	6	1	0	0	1	0	0	1	1	1	1	0	20.02.2012	15.01.2020	-3.6	13.89	0
BAL	GAC	2	NO-FIL	TDX/TDX	6	1	0	0	1	0	1	1	0	0	1	0	20.02.2012	15.01.2020	-19	137.67	0
BAL	GAC	2	NO-GAP	TDX/TDX	6	1	0	0	1	0	1	1	0	0	1	0	20.02.2012	15.01.2020	-3.48	17.5	0
BAL	GAC	2	NO-PEN	TDX/TDX	6	1	0	0	1	0	1	1	1	1	0	0	20.02.2012	15.01.2020	-3.18	14.13	0
BAL	GAC	1	SEAS	TDX/TDX	6	1	0	0	1	0	1	1	1	1	1	0	20.02.2012	15.01.2020	-3.53	14.06	0
BAL	FAU	1	CTL	ASTER/ASTER	30	1	0	0	1	0	1	1	1	1	0	0	28.03.2011	26.07.2020	-4.05	0.142	1
BAL	FAU	3	CTL	TDX/TDX	6	1	0	0	1	0	1	1	1	1	0	0	09.02.2012	18.09.2018	-0.398	0.079	1
BAL	FAU	3	NO-CO	TDX/TDX	6	1	0	0	1	0	0	1	1	1	0	0	09.02.2012	18.09.2018	7.411	0.659	0
BAL	FAU	3	NO-FIL	TDX/TDX	6	1	0	0	1	0	1	1	0	1	0	0	09.02.2012	18.09.2018	-0.466	0.079	0
BAL	FAU	3	NO-GAP	TDX/TDX	6	1	0	0	1	0	1	1	1	0	0	0	09.02.2012	18.09.2018	-0.308	0.079	0
BAL	TAR	2															01.10.2011	01.10.2019			

Table S21. Experiment results for the eastern part of the Northern Patagonian Icefield (NPI) for the target period from 2000 to 2014.

For each group and run, a summary of data and workflow (0: no; 1: yes) is provided together with survey dates (DD.MM.YYYY) and corresponding elevation changes (dh) in metre.

Uncertainties are reported in metre and at 95% confidence levels. Results reported as low confidence as well as sensitivity runs (e.g., NO-CO: no co-registration) have a quality flag of 0.

Start and end dates of the target period (TAR) are given in the last row.

GLACIER	GROUP	RUN	RUN_NAME	SOURCE	DEM_COUNT	PROVIDED	PROCESSED	PAIR	MOSAIC	TIMESERIES	CO-REGISTRATION	BIAS	NOISE_FILTERING	VOID_FILLING	PENETRATION	TEMPORAL	START_DATE	END_DATE	dh	dh_UNCERTAINTY	QUALITY_FLAG
NPI	ETH	1	CTL	ASTER/ASTER		0	1	0	0	1	1	1	1	1	0	1	01.02.2000	01.03.2014	-12.843	4.337	1
NPI	FAU	1	CTL	SRTM/TDX		1	0	0	1	0	1	1	1	1	0	0	16.02.2000	16.04.2014	-11.045	0.099	1
NPI	UST	1	CTL	SRTM/ASTER		1	0	0	1	0	1	1	1	1	0	0	16.02.2000	24.03.2014	-13.992	5.816	1
NPI	UST	2	CTL	SRTM/ASTER		1	0	0	1	0	1	1	1	1	0	0	16.02.2000	24.03.2014	-13.35	5.816	1
NPI	UST	3	CTL	SRTM/ASTER		1	0	0	1	0	1	1	1	1	0	0	16.02.2000	24.03.2014	-15.509	5.816	1
NPI	UST	4	CTL	SRTM/ASTER		1	0	0	1	0	1	1	1	1	0	0	16.02.2000	24.03.2014	-15.853	5.816	1
NPI	UST	1	NO-BIAS/NO-OUTL/NO-FIL	SRTM/ASTER		1	0	0	1	0	1	0	0	0	0	0	16.02.2000	24.03.2014	-7.781	5.949	0
NPI	UST	1	NOFIL	SRTM/ASTER		1	0	0	1	0	1	1	0	1	0	0	16.02.2000	24.03.2014	-10.055	5.816	0
NPI	UGA	1	CTL	ASTER/ASTER		1	0	0	0	1	1	1	1	1	0	1	02.05.2000	07.04.2014	-14.934	0.85	1
NPI	UGA	2	CTL	ASTER/ASTER		1	0	0	0	1	1	1	1	1	0	1	02.05.2000	25.03.2021	-17.02	0.779	1
NPI	UGA	1	NO-BIAS	ASTER/ASTER		1	0	0	0	1	1	0	1	1	0	1	02.05.2000	07.04.2014	-15.334	0.954	0
NPI	UGA	1	NO-CO	ASTER/ASTER		1	0	0	0	1	0	1	1	1	0	1	02.05.2000	07.04.2014	-33.592	1.9	0
NPI	UGA	1	NO-FILT	ASTER/ASTER		1	0	0	0	1	1	1	0	1	0	1	02.05.2000	07.04.2014	-14.93	0.85	0
NPI	UGA	1	NO-GAP	ASTER/ASTER		1	0	0	0	1	1	1	1	0	0	1	02.05.2000	07.04.2014	-16.073	0.88	0
NPI	TAR	1															01.02.2000	01.03.2014			

Table S22. Experiment results for the eastern part of the Northern Patagonian Icefield (NPI) for the target period from 2014 to 2019.

For each group and run, a summary of data and workflow (0: no; 1: yes) is provided together with survey dates (DD.MM.YYYY) and corresponding elevation changes (dh) in metre.

Uncertainties are reported in metre and at 95% confidence levels. Results reported as low confidence as well as sensitivity runs (e.g., NO-CO: no co-registration) have a quality flag of 0.

Start and end dates of the target period (TAR) are given in the last row.

GLACIER	GROUP	RUN	RUN_NAME	SOURCE	DEM_COUNT	PROVIDED	PROCESSED	PAIR	MOSAIC	TIMESERIES	CO-REGISTRATION	BIAS	NOISE_FILTERING	VOID_FILLING	PENETRATION	TEMPORAL	START_DATE	END_DATE	dh	dh_UNCERTAINTY	QUALITY_FLAG
NPI	ETH	1	CTL	ASTER/ASTER		0	1	0	0	1	1	1	1	1	0	1	01.03.2014	01.03.2019	-6.725	3.393	1
NPI	FAU	2	CTL	TDX/TDX		1	0	0	1	0	1	1	1	1	0	0	16.04.2014	30.03.2019	-8.201	0.076	1
NPI	UST	5	CTL	ASTER/TDX	5	1	0	0	1	0	1	1	1	1	0	0	24.03.2014	04.03.2019	-6.845	4.169	1
NPI	UST	6	CTL	ASTER/TDX	5	1	0	0	1	0	1	1	1	1	0	0	24.03.2014	04.03.2019	-6.993	4.169	1
NPI	UST	7	CTL	ASTER/TDX	5	1	0	0	1	0	1	1	1	1	0	0	24.03.2014	04.03.2019	-7.354	4.169	1
NPI	UST	8	CTL	ASTER/TDX	5	1	0	0	1	0	1	1	1	1	0	0	24.03.2014	04.03.2019	-7.346	4.169	1
NPI	UST	5	NO-BIAS/NO-OUTL/NO-FIL	ASTER/TDX	5	1	0	0	1	0	1	0	0	0	0	0	24.03.2014	04.03.2019	-2.732	4.753	0
NPI	UST	5	NOFIL	ASTER/TDX	5	1	0	0	1	0	1	1	0	0	0	0	24.03.2014	04.03.2019	-6.505	4.169	0
NPI	UGA	1	CTL	ASTER/ASTER		1	0	0	0	1	1	1	1	1	0	1	07.04.2014	21.02.2020	-7.868	0.578	1
NPI	UGA	2	CTL	ASTER/ASTER		1	0	0	0	1	1	1	1	1	0	1	07.04.2014	25.03.2021	-6.057	0.277	1
NPI	UGA	1	NO-BIAS	ASTER/ASTER		1	0	0	0	1	1	0	1	1	0	1	07.04.2014	21.02.2020	-7.848	0.578	0
NPI	UGA	1	NO-CO	ASTER/ASTER		1	0	0	0	1	0	1	1	1	0	1	07.04.2014	21.02.2020	-14.783	1.13	0
NPI	UGA	1	NO-FILT	ASTER/ASTER		1	0	0	0	1	1	1	0	1	0	1	07.04.2014	21.02.2020	-7.867	0.578	0
NPI	UGA	1	NO-GAP	ASTER/ASTER		1	0	0	0	1	1	1	1	0	0	1	07.04.2014	21.02.2020	-8.947	0.603	0
NPI	TAR	2															01.03.2014	01.03.2019			

References

- Abdel Jaber, W., Rott, H., Floricioiu, D., Wuite, J., and Miranda, N.: Heterogeneous spatial and temporal pattern of surface elevation change and mass balance of the Patagonian ice fields between 2000 and 2016, *The Cryosphere*, 13, 2511–2535, <https://doi.org/10.5194/tc-13-2511-2019>, 2019.
- Agarwal, V., Bolch, T., Syed, T. H., Pieczonka, T., Strozzi, T., and Nagaich, R.: Area and mass changes of Siachen Glacier (East Karakoram), *J. Glaciol.*, 63, 148–163, <https://doi.org/10.1017/jog.2016.127>, 2017.
- Berthier, E., Vincent, C., Magnússon, E., Gunnlaugsson, Á. Þ., Pitte, P., Le Meur, E., Masiokas, M., Ruiz, L., Pálsson, F., Belart, J. M. C., and Wagnon, P.: Glacier topography and elevation changes derived from Pléiades sub-meter stereo images, *The Cryosphere*, 8, 2275–2291, <https://doi.org/10.5194/tc-8-2275-2014>, 2014.
- Berthier, E., Cabot, V., Vincent, C., and Six, D.: Decadal Region-Wide and Glacier-Wide Mass Balances Derived from Multi-Temporal ASTER Satellite Digital Elevation Models. Validation over the Mont-Blanc Area, *Front. Earth Sci.*, 4, <https://doi.org/10.3389/feart.2016.00063>, 2016.
- Bollmann, E., Girmair, A., Mitterer, S., Krainer, K., Sailer, R., and Stötter, J.: A Rock Glacier Activity Index Based on Rock Glacier Thickness Changes and Displacement Rates Derived From Airborne Laser Scanning: Rock Glacier Activity Index, *Permafrost and Periglac. Process.*, 26, 347–359, <https://doi.org/10.1002/ppp.1852>, 2015.
- Buchhorn, M., Lesiv, M., Tsendbazar, N.-E., Herold, M., Bertels, L., and Smets, B.: Copernicus Global Land Cover Layers—Collection 2, *Remote Sensing*, 12, 1044, <https://doi.org/10.3390/rs12061044>, 2020.
- Dussaillant, I., Berthier, E., Brun, F., Masiokas, M., Hugonnet, R., Favier, V., Rabatel, A., Pitte, P., and Ruiz, L.: Two decades of glacier mass loss along the Andes, *Nat. Geosci.*, 12, 802–808, <https://doi.org/10.1038/s41561-019-0432-5>, 2019.
- Dussaillant, I., Bannwart, J., Paul, F., and Zemp, M.: Glacier mass change global gridded data from 1976 to present derived from the Fluctuations of Glaciers Database., *World Glacier Monitoring Service*, 2023.
- Fischer, M., Huss, M., and Hoelzle, M.: Surface elevation and mass changes of all Swiss glaciers 1980–2010, *The Cryosphere*, 9, 525–540, <https://doi.org/10.5194/tc-9-525-2015>, 2015.
- Fritz, T., Rossi, C., Yague-Martinez, N., Rodriguez-Gonzalez, F., Lachaise, M., and Breit, H.: Interferometric processing of TanDEM-X data, in: 2011 IEEE International Geoscience and Remote Sensing Symposium, IGARSS 2011 - 2011 IEEE International Geoscience and Remote Sensing Symposium, Vancouver, BC, Canada, 2428–2431, <https://doi.org/10.1109/IGARSS.2011.6049701>, 2011.
- Gardelle, J., Berthier, E., Arnaud, Y., and Käab, A.: Region-wide glacier mass balances over the Pamir-Karakoram-Himalaya during 1999–2011, *The Cryosphere*, 7, 1263–1286, <https://doi.org/10.5194/tc-7-1263-2013>, 2013.
- Girod, L., Nuth, C., Käab, A., McNabb, R., and Galland, O.: MMASTER: Improved ASTER DEMs for Elevation Change Monitoring, *Remote Sensing*, 9, 704, <https://doi.org/10.3390/rs9070704>, 2017.
- González, C., Bachmann, M., Bueso-Bello, J.-L., Rizzoli, P., and Zink, M.: A Fully Automatic Algorithm for Editing the TanDEM-X Global DEM, *Remote Sensing*, 12, 3961, <https://doi.org/10.3390/rs12233961>, 2020.
- Guillet, G. and Bolch, T.: Bayesian estimation of glacier surface elevation changes from DEMs. *Frontiers in Earth Science*, 11, p.1076732, <https://doi.org/10.3389/feart.2023.1076732>, 2023

- Höhle, J. and Höhle, M.: Accuracy assessment of digital elevation models by means of robust statistical methods, *ISPRS Journal of Photogrammetry and Remote Sensing*, 64, 398–406, <https://doi.org/10.1016/j.isprsjprs.2009.02.003>, 2009.
- Hugonnet, R., McNabb, R., Berthier, E., Menounos, B., Nuth, C., Girod, L., Farinotti, D., Huss, M., Dussaillant, I., Brun, F., and Kääb, A.: Accelerated global glacier mass loss in the early twenty-first century, *Nature*, 592, 726–731, <https://doi.org/10.1038/s41586-021-03436-z>, 2021.
- Hugonnet, R., Brun, F., Berthier, E., Dehecq, A., Mannerfelt, E. S., Eckert, N., and Farinotti, D.: Uncertainty Analysis of Digital Elevation Models by Spatial Inference From Stable Terrain, *IEEE J. Sel. Top. Appl. Earth Observations Remote Sensing*, 15, 6456–6472, <https://doi.org/10.1109/JSTARS.2022.3188922>, 2022.
- Kumar, A., Dasgupta, A., Lokhande, S., and Ramsankaran, R.: Benchmarking the Indian National CartoDEM against SRTM for 1D hydraulic modelling, *International Journal of River Basin Management*, 17, 479–488, <https://doi.org/10.1080/15715124.2019.1606816>, 2019.
- Lin, H., Li, G., Cuo, L., Hooper, A., and Ye, Q.: A decreasing glacier mass balance gradient from the edge of the Upper Tarim Basin to the Karakoram during 2000–2014, *Sci Rep*, 7, 6712, <https://doi.org/10.1038/s41598-017-07133-8>, 2017.
- Magnússon, E., Muñoz-Cobo Belart, J., Pálsson, F., Ágústsson, H., and Crochet, P.: Geodetic mass balance record with rigorous uncertainty estimates deduced from aerial photographs and lidar data – Case study from Drangajökull ice cap, NW Iceland, *The Cryosphere*, 10, 159–177, <https://doi.org/10.5194/tc-10-159-2016>, 2016.
- McNabb, R., Nuth, C., Kääb, A., and Girod, L.: Sensitivity of glacier volume change estimation to DEM void interpolation, *The Cryosphere*, 13, 895–910, <https://doi.org/10.5194/tc-13-895-2019>, 2019.
- McNeil, C., O’Neel, S., Loso, M., Pelto, M., Sass, L., Baker, E. H., and Campbell, S.: Explaining mass balance and retreat dichotomies at Taku and Lemon Creek Glaciers, Alaska, *J. Glaciol.*, 66, 530–542, <https://doi.org/10.1017/jog.2020.22>, 2020.
- Nuth, C. and Kääb, A.: Co-registration and bias corrections of satellite elevation data sets for quantifying glacier thickness change, *The Cryosphere*, 5, 271–290, <https://doi.org/10.5194/tc-5-271-2011>, 2011.
- O’Neel, S., McNeil, C., Sass, L. C., Florentine, C., Baker, E. H., Peitzsch, E., McGrath, D., Fountain, A. G., and Fagre, D.: Reanalysis of the US Geological Survey Benchmark Glaciers: long-term insight into climate forcing of glacier mass balance, *J. Glaciol.*, 65, 850–866, <https://doi.org/10.1017/jog.2019.66>, 2019.
- Paul, F., Barrand, N. E., Baumann, S., Berthier, E., Bolch, T., Casey, K., Frey, H., Joshi, S. P., Konovalov, V., Le Bris, R., Mölg, N., Nosenko, G., Nuth, C., Pope, A., Racoviteanu, A., Rastner, P., Raup, B., Scharrer, K., Steffen, S., and Winsvold, S.: On the accuracy of glacier outlines derived from remote-sensing data, *Ann. Glaciol.*, 54, 171–182, <https://doi.org/10.3189/2013AoG63A296>, 2013.
- Pfeifer, N., Mandlbürger, G., Otepka, J., and Karel, W.: OPALS – A framework for Airborne Laser Scanning data analysis, *Computers, Environment and Urban Systems*, 45, 125–136, <https://doi.org/10.1016/j.compenvurbsys.2013.11.002>, 2014.
- Pieczonka, T. and Bolch, T.: Region-wide glacier mass budgets and area changes for the Central Tien Shan between ~1975 and 1999 using Hexagon KH-9 imagery, *Global and Planetary Change*, 128, 1–13, <https://doi.org/10.1016/j.gloplacha.2014.11.014>, 2015.
- RGI Consortium: Randolph Glacier Inventory - a dataset of global glacier outlines: version 6.0, technical report., Global Land Ice Measurements from Space, Colorado, USA. Digital Media. DOI: 10.7265/N5-RGI-60, 2017.

Rolstad, C., Haug, T., and Denby, B.: Spatially integrated geodetic glacier mass balance and its uncertainty based on geostatistical analysis: application to the western Svartisen ice cap, Norway, *J. Glaciol.*, 55, 666–680, <https://doi.org/10.3189/002214309789470950>, 2009.

Schweisshelm, B., Lachaise, M., and Fritz, T.: Change Detection Within the Processing of the TanDEM-X Change DEM, in: 2021 IEEE International Geoscience and Remote Sensing Symposium IGARSS, IGARSS 2021 - 2021 IEEE International Geoscience and Remote Sensing Symposium, Brussels, Belgium, 2130–2133, <https://doi.org/10.1109/IGARSS47720.2021.9554010>, 2021.

Shean, D. E., Alexandrov, O., Moratto, Z. M., Smith, B. E., Joughin, I. R., Porter, C., and Morin, P.: An automated, open-source pipeline for mass production of digital elevation models (DEMs) from very-high-resolution commercial stereo satellite imagery, *ISPRS Journal of Photogrammetry and Remote Sensing*, 116, 101–117, <https://doi.org/10.1016/j.isprsjprs.2016.03.012>, 2016.

Wagnon, P., Brun, F., Khadka, A., Berthier, E., Shrestha, D., Vincent, C., Arnaud, Y., Six, D., Dehecq, A., Ménégoz, M., and Jomelli, V.: Reanalysing the 2007–19 glaciological mass-balance series of Mera Glacier, Nepal, Central Himalaya, using geodetic mass balance, *J. Glaciol.*, 67, 117–125, <https://doi.org/10.1017/jog.2020.88>, 2021.

Zemp, M., Jansson, P., Holmlund, P., Gärtner-Roer, I., Koblet, T., Thee, P., and Haeberli, W.: Reanalysis of multi-temporal aerial images of Storglaciären, Sweden (1959–99) – Part 2: Comparison of glaciological and volumetric mass balances, *The Cryosphere*, 4, 345–357, <https://doi.org/10.5194/tc-4-345-2010>, 2010.

Zemp, M., Huss, M., Thibert, E., Eckert, N., McNabb, R., Huber, J., Barandun, M., Machguth, H., Nussbaumer, S. U., Gärtner-Roer, I., Thomson, L., Paul, F., Maussion, F., Kutuzov, S., and Cogley, J. G.: Global glacier mass changes and their contributions to sea-level rise from 1961 to 2016, *Nature*, 568, 382–386, <https://doi.org/10.1038/s41586-019-1071-0>, 2019.